UNIVERSITY OF DEBRECEN
FACULTY OF ENGINEERING
DEPARTMENT OF
MECHANICAL ENGINEERING

OPTICAL STRESS FIELD MEASUREMENT DEVICE DEVELOPMENT

THESIS

Carlos Emilio Bonilla Barragán
Production Engineering Specialization

Debrecen
2025

Table of Contents

Table of Figures

Table of Tables

Table of Notations

σ	$[Pa]$	Stress
F	[N]	Force
M	[Nm]	Momentum
ε	$[-]$	Strain
E	[Pa]	Modulus of elasticity
δ	[mm]	Deflection
W	$[mm^3]$	Section modulus
I	$[kgm^2]$	Inertia

1 Introduction

Materials and their properties have gained a lot of relevance over the years, making it more present in our daily lives than it seems. A large part of our lives is to a greater or lesser extent influenced by materials, both in transportation, telecommunications, housing, clothing, etc. Over the years, thousands of different materials have been designed and manufactured with unique and very specific characteristics to meet the needs we have daily, various types of metals, plastics, paper, even food and special fibers.

The advancement of technology that makes our lives easier is closely related to the access we have to appropriate materials. Many technologies have advanced by leaps and bound thanks to the development of some material. Knowing the mechanical properties of materials is important to understand how they will perform, how reliable they will be, and how effective they will become in certain applications.

Traditionally, the study of materials, both analyzing their mechanical stresses and deformations, has been achieved through analog techniques which have allowed a great advance as it would be with the use of strain gauges, sensors, and other traditional measuring devices, despite having been fundamental in the past, they are lagging in the face of new technologies that solve the limitations that they had as well as with a higher resolution, greater sensitivity, allowing us to measure in real time without much effort, etc. and mainly being able to work with advanced materials and geometries that with analog technology we could not analyze correctly.

Currently, advances in optics, sensors and computing capacity have led to the appearance of new non-contact, non-invasive and non-destructive measurement techniques, such as DIC or Digital Image Correlation. This new technology makes it possible to carry out high-precision strain measurements in a non-intrusive way, in real time and over the entire study surface. These types of technologies are relevant for industries that require the development of new materials, with complex geometries and dynamics with high efficiency and long life.

Although there is commercial DIC equipment, it is still inaccessible and not very customizable for many companies that need to speed up their development times and adapt their operations to new technologies that allow them to perform mechanical tests while obtaining high-resolution data and images which allow them to analyze stresses and deformations optimally and in real time.

The objective of this study is to develop a device capable of performing stress measurements, more specifically, bending tests in a traditional way, using gauges and sensors, and with real-time verification by DIC. This includes the development

of 3-point clamping jigs for bending tests, the adaptation of an old durometer frame for use as a loading device (approx. 300 N), the design of supports for a camera-lighting system optimized for obtaining high-resolution images, the development of software that allows tests to be carried out on the device and obtain analyzable, replicable and comparable results to then process the data obtained. It should be noted that the aim is for the entire device to be optimized with specific dimensions to make it maneuverable if required.

2 Literature Review

The relevance of materials in our daily lives is more important every day than one imagines. Practically everything around us was made with some material which was designed to fulfill that specific function, whether it is the steel of the columns of a building to a paper sleeve which we use to buy our things in stores. We live surrounded by a lot of advanced technology that we ignore just because we see it every day, it seems very simple, or simply, it does not attract much attention but that perfectly fulfill the function for which they were designed.

Materials when they are in use are subjected to loads and forces constantly, in real life a static condition is very complicated, so you have to be prepared and know the properties and unique characteristics of each material used which allows us to design a part, which when faced with a change or a deformation, this will not excessive and does not cause a failure or breakage in our material.

Often, we want to know several aspects that affect the behavior of a material, so the study of the forces, moments and stresses to which they are subjected becomes relevant [14]. A tensile or compression test allows us to know many properties of materials, however, they do not provide all the necessary information.

Bending tests provide us with data on the strength, stiffness and toughness of a material, and are particularly useful when the material is to be used as a support structure [15].

2.1 Bending Stress

The bending stress appears in very diverse situations, being decisive in the behavior of structures or parts. For this reason, it is necessary to know it in order to correctly carry out any design.

2.1.1 Pure Bending

Considering a beam to which two equal turning moments are applied but in the opposite direction at its ends. This situation is known as pure bending, because there are no other types of loads or forces applied to the beam, and therefore, there are no shear forces.

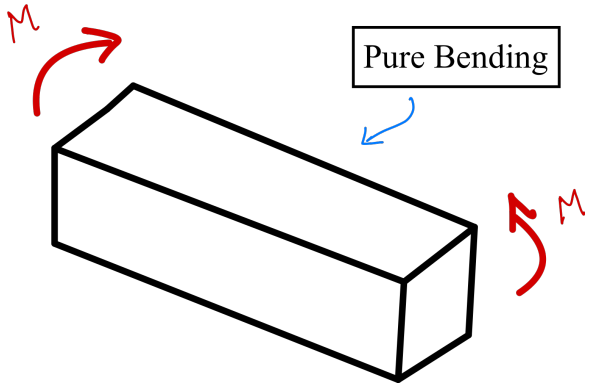

Figure 1 Pure bending diagram.

In this situation, the beam undergoes a deformation causing it to flex, bending due to the effect of the applied turning moments. As can be seen in the figure, the upper fibers shorten their length, that is, they are compressed; while the lower fibers are elongated, that is, they are traction. With which there will be a transition from the upper part to the lower part, finding the neutral line, which is the one that does not suffer traction or compressive stresses, its length being equal to the initial length of the beam because it does not deform [13].

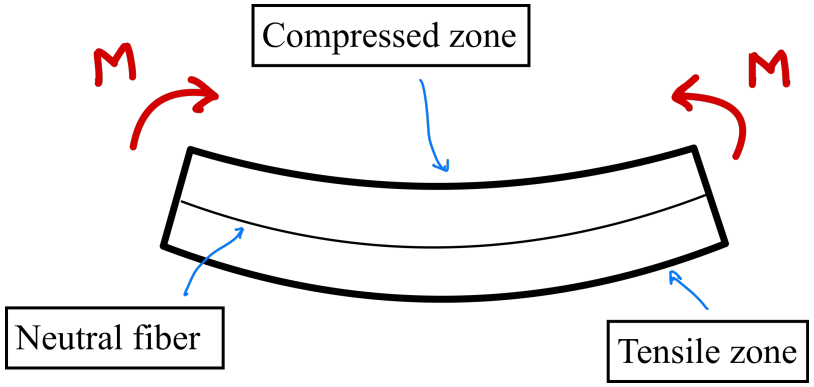

Figure 2 Zones distribution in pure bending.

The neutral fiber is located in the centroid of the cross-section of the beam and separates both zones, in other words. the compressed zone from the tensile zone [13].

Cross-Section of the Bar

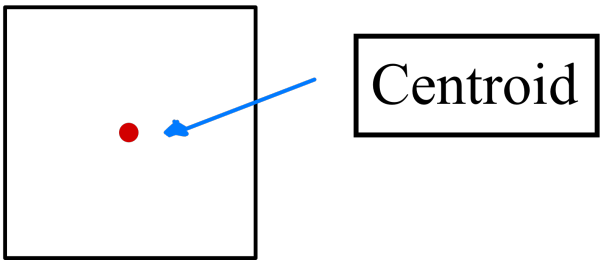

Figure 3 Cross-section of the beam.

Tensile and compressive stresses cause axial stresses to be generated, perpendicular to the beam section [1].

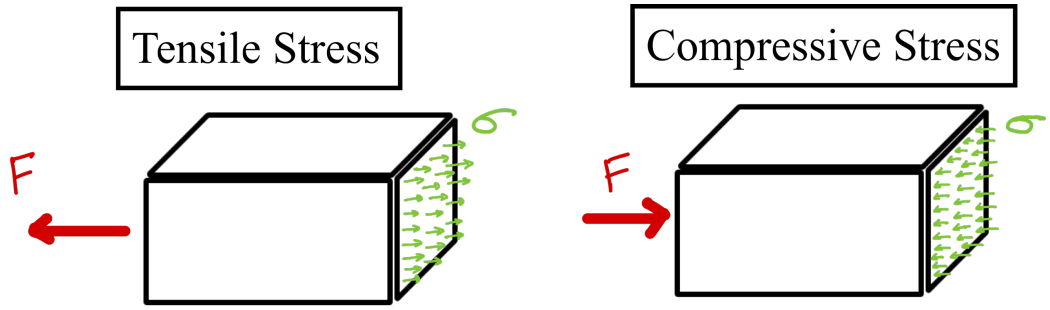

Figure 4 Tensile and compressive stresses

By making a cut in the beam in any section we can analyze what happens to the bending at this point. In order to maintain static equilibrium, normal stress appears, but unlike for simple cases of compression or traction, the bending effort does not generate a constant normal stress throughout the section, but this will vary with distance until it reaches the neutral fiber, with the maximum stress at the ends of the beam and clearly distinguishing the compressed and tensile areas [2]. In neutral fiber the stress is zero.

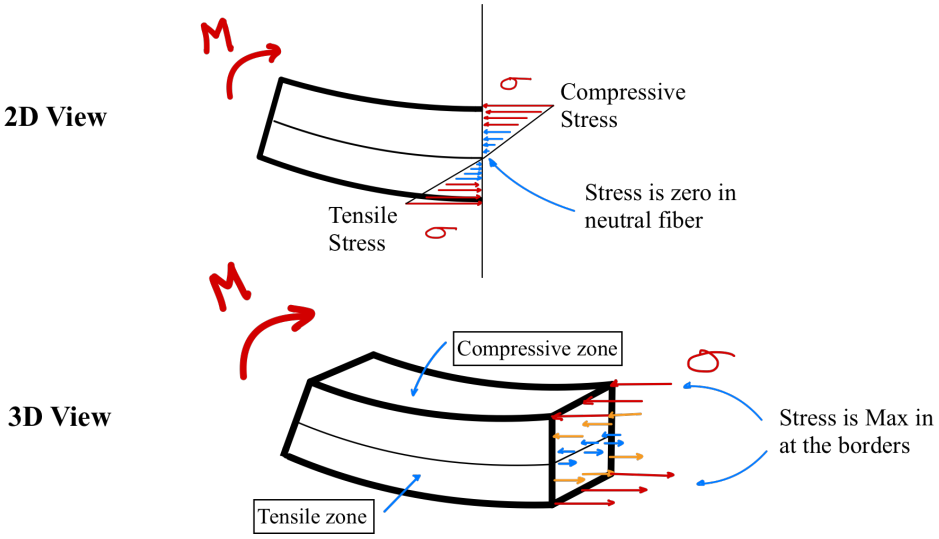

Figure 5 Stress distribution during pure bending.

2.1.2 Calculating the Stress for Each Fiber Inside the Beam

We are going to consider a curved beam because of the turning moments applied to its ends. The beam follows a curvature around a center of rotation O, we have also R which will be the distance between the center of rotation and the position of the neutral fiber of the beam, remember that the length of the neutral fiber has not varied with respect to the length of the beam.

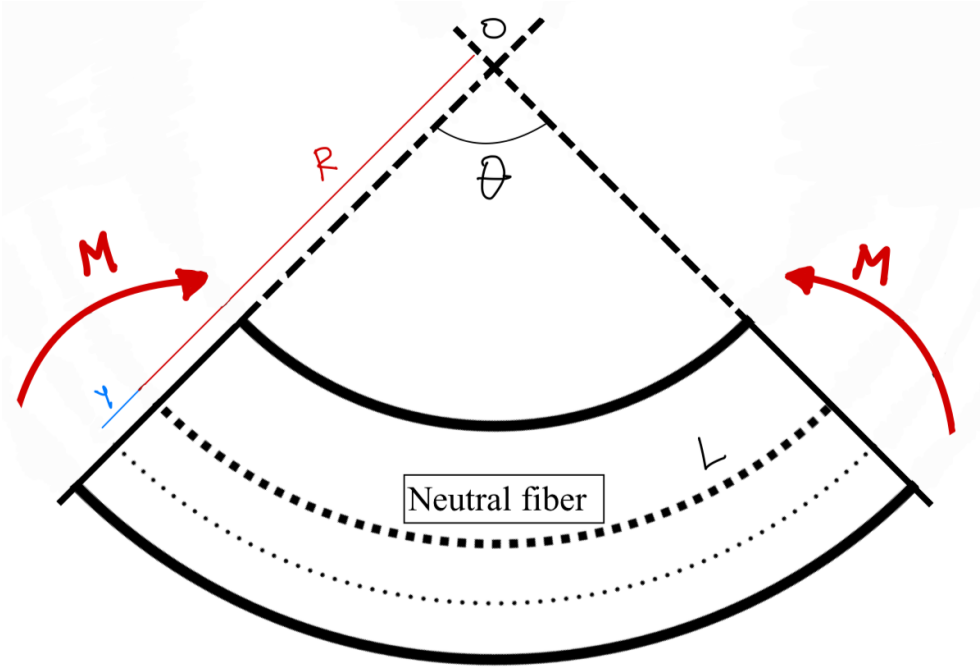

Figure 6 Figure for stress calculating in a fiber with a distance y of the neutral fiber.

With this in mind, it's possible to deduce that the initial length of the beam L will be R times the theta angle.

$$L = R * \theta \tag{1}$$

Similarly, any fiber displaced within the beam by a distance y from the neutral fiber will now measure a length of L_2 equal to distance R added to the distance y multiplied by the Theta angle [2].

$$L_2 = (R + y) * \theta \tag{2}$$

However, we know that initially all the fibers of the beam used to have the same length before the turning moments were applied, so applying the concept of deformation, such that:

$$\varepsilon = \frac{\Delta L}{L} \tag{3}$$

We can calculate the deformation of this fiber as the increase in length between its initial length.

$$\varepsilon = \frac{(R + y) * \theta - R * \theta}{R * \theta}$$

$$\varepsilon = \frac{y}{R} \tag{4}$$

Hooke's law relates normal stress to normal strain [1].

$$\sigma = E * \varepsilon \tag{5}$$

Being E the elastic modulus of the material.

If we replace Hooke's law in the deformation equation, we can calculate the stress produced by the bending stress as a function of distance y to neutral fiber.

$$\sigma = \frac{E * y}{R} \tag{6}$$

However, this expression depends on the radius R which is a consequence of the deformation produced by the moment applied, making it impractical. To solve this, it is more convenient to obtain an expression of the stress as a function of momentum [2].

Considering again a section of the beam, when it is in equilibrium, the rotation caused by the moment M will be balanced by the effect of normal stress. On each differential element of the section, that is, on each minimum section located at a distance y an applied stress will appear on the neutral fiber that generates a turning moment contrary to the moment M. The sum of these moments will be equal to the moment applied [2].

$$M = \sum \sigma * y * dA \tag{7}$$

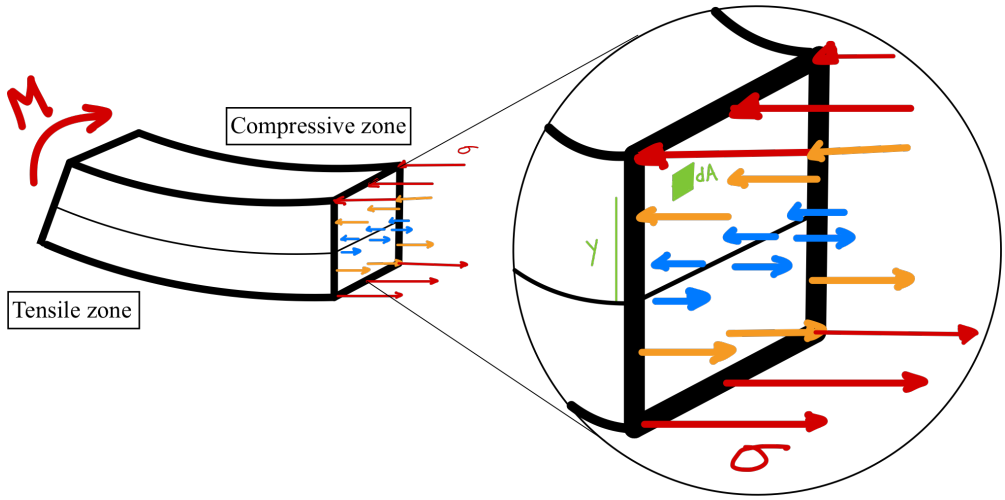

Figure 7 Diagram of a differential element stresses distribution.

This can also be shown as a surface integral where the stress σ It can be replaced by the expression previously found and we can notice how the integral resulting from this expression coincides with the definition of second moment of inertia [3].

$$M = \int_S \sigma * y * dA \tag{8}$$

$$M = \int_S \frac{E}{R} * y^2 * dA$$

$$M = \frac{E}{R} \int_S y^2 dA$$

$$M = \frac{E}{R} * I \tag{9}$$

The second moment of inertia is related to the geometric resistance of the profile to the bending stress [3]. Finally, replacing the expression of σ In the equation we obtain the normal stress produced as a function of momentum M applied, the position y with respect to the neutral fiber, and the moment of inertia of the section.

$$\sigma = \frac{M * y}{I} \tag{10}$$

The normal stress sign is positive in the betrayed area and negative in the compressed area and will depend on the direction in which we move with respect to the neutral fiber [2].

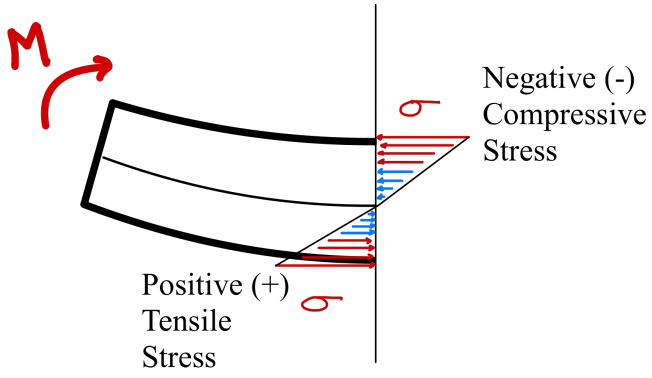

Figure 8 Sign distribution for normal stresses.

The maximum stress will be the stress calculated at the ends furthest from the neutral fiber, in other words. in the point with the distance y_{max}. The elastic resistant modulus of a section can be defined as the difference in the moment of inertia between the distance y_{max} [1].

$$W = \frac{I}{y_{max}} \tag{11}$$

Therefore, the maximum stress is obtained directly from the difference between the applied moment and the elastic resistant modulus.

$$\sigma_{max} = \frac{M}{W} \tag{12}$$

It should be remembered that bending does not usually act alone, is usually accompanied by traction, compression and shear stresses; these being also necessary to take into consideration when designing [1].

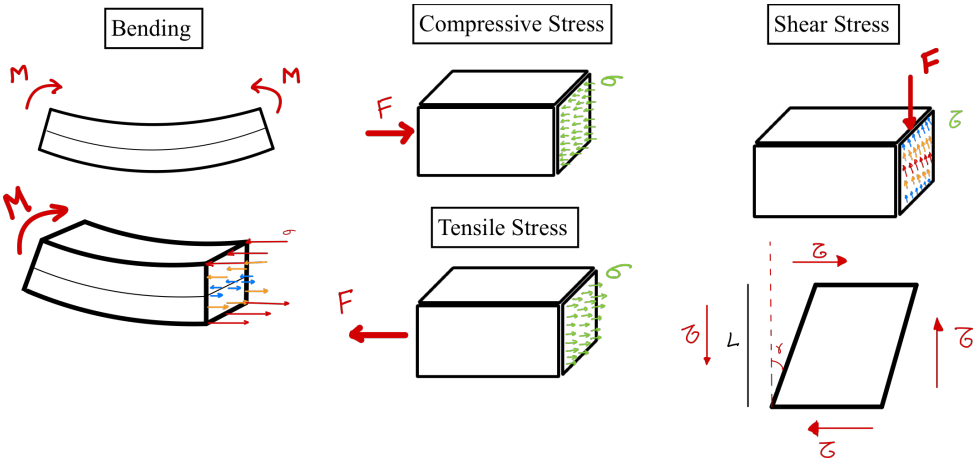

Figure 9 Stresses acting in a beam.

2.2 Bending Test

The bending test is a static test, that is, at a very low deformation speed and with controlled conditions, which allows us to know the mechanical properties of the materials. This type of test can be performed on a universal testing machine or on a dynamic fatigue testing system [4]. Bending tests allow the behavior of materials to be measured under the load of a single beam.

When a material is bent or flexed, it is subject to a combination of tensile, compressive and shear forces. That is why a bending test is carried out, which imitates realistic load situations. A bending test is performed with a 3- or 4-point bending fixture that applies force in different ways according to the configuration [14].

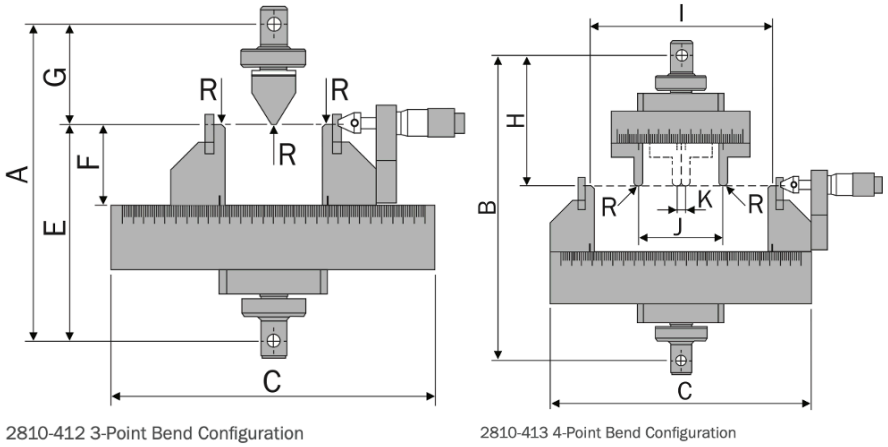

Figure 10 Point-bend configuration of an Instron 2810 Series Mini Flexure Fixture. (Source: [5])

In the three-point bending test, a cylindrical or prismatic specimen is placed on two supports by applying a punch load to the center. As the applied force increases, the specimen undergoes a greater bending stress.

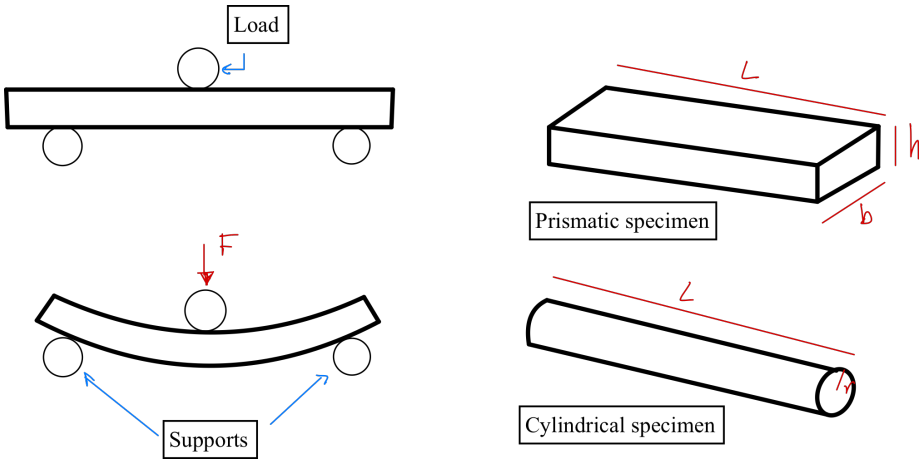

Figure 11 Specimen and load configuration for a bending test.

Depending on the requirements, a material can be tested up to a certain load or strain limit, or until the specimen breaks. Bending stress, bending deformation, flexural modulus, and displaced bending yield limit can be measured [4].

2.2.1 Theory Behind Bending Testing

Considering the specimen as a double-supported beam, and analyzing the moments, we observe that it is subjected to a bending moment that is maximum in the central section. If the charge F is applied in the center, it can be deduced that the reactions in both supports correspond to half of the charge. As the distance to the center is half that of the distance between the supports, the value of the maximum bending moment is obtained.

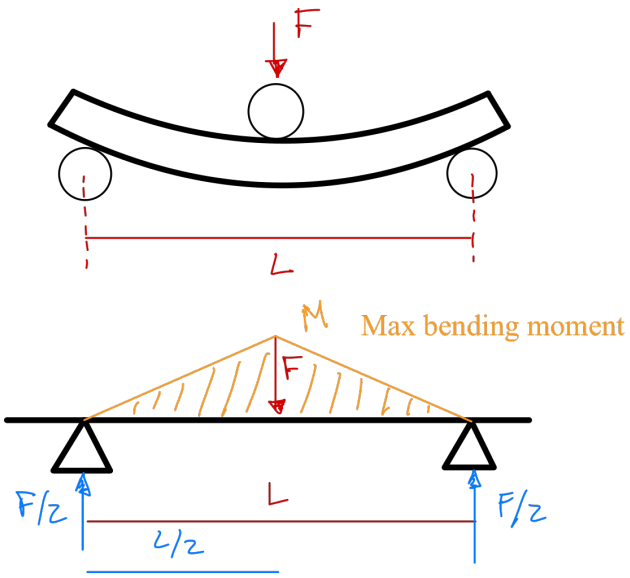

Figure 12 Diagram of forces and moments on the beam.

$$M = \frac{F}{2} * \frac{L}{2}$$

$$M = \frac{F * L}{4} \tag{13}$$

As mentioned before, this moment generates a compressed upper zone, which measures less than the original length without deforming; and a tensile lower zone, of greater length. Both zones are separated by the neutral axis in the center of the specimen, which does not change its length because it does not deform [13]. This situation generates a linear axial stress distribution from the maximum compressive stress to the maximum tensile stress, both in the extreme fibers of the section, with a stress of zero in the position of the neutral axis.

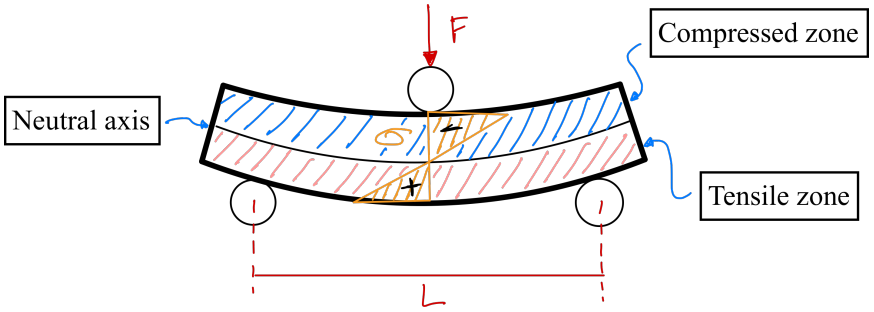

Figure 13 Stress distribution on the beam during a bending test.

The stress distribution can be defined as a function of the applied bending moment with respect to the moment of inertia of the section and the position of the analyzed from the neutral axis, as explained previously in the obtaining of equation 10.

$$\sigma = \frac{M}{I} * z \tag{14}$$

The maximum stress, both tensile and compressive, will occur in the extreme fibers. As explained in obtaining equation 12 and substituting the distance z, the maximum stress value is deduced as a function of the applied moment and the elastic resistant modulus of the section, which is a geometric property [6].

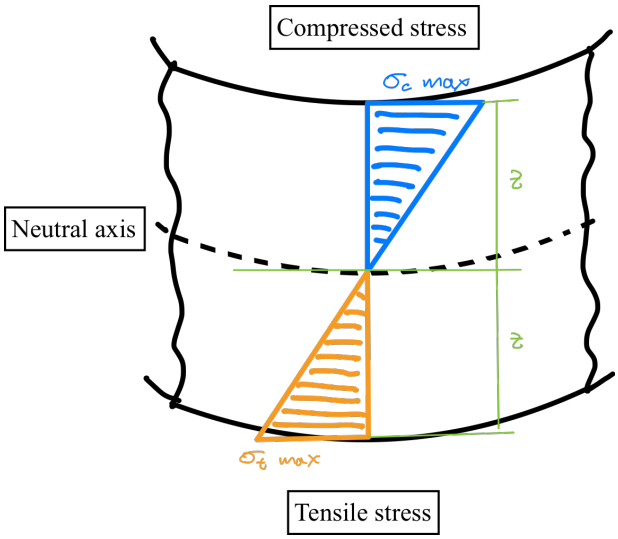

Figure 14 Max stresses.

$$\sigma_{max} = \frac{M}{I} * z$$

$$\sigma_{max} = \frac{M}{I/z}$$

$$\sigma_{max} = \frac{M}{W_{el}} \tag{15}$$

Where we also know that

$$M = \frac{F * L}{4} \tag{16}$$

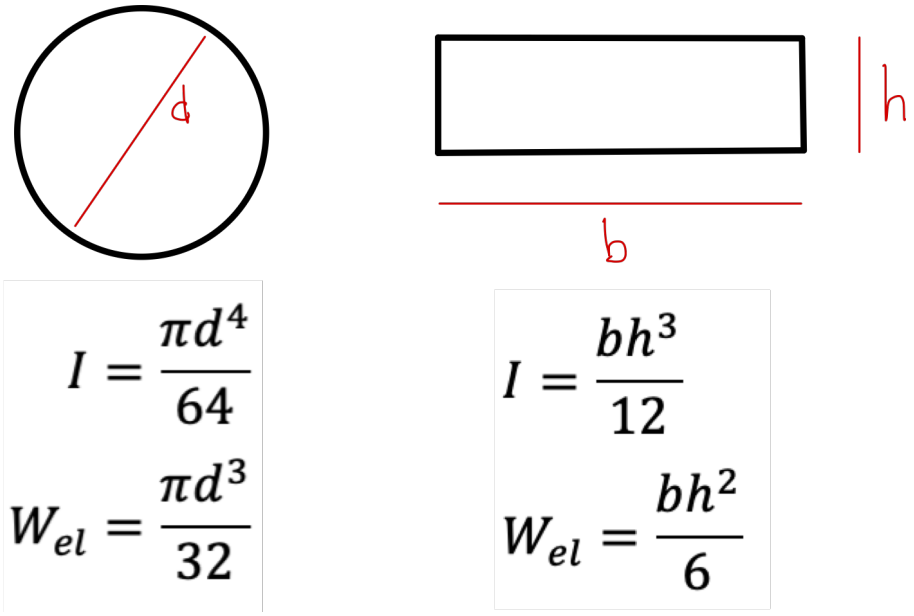

Figure 15 Applied moment and the elastic resistant modulus of the section.

This means that, depending on the length between supports, the applied load and the geometry of the specimen, the maximum stress the material is under during the test is known.

However, these equations are only valid in the elastic zone of the material, when the deformations are reversible. When the elastic limit of the material is exceeded, the material begins to plasticize, causing the relationship between stress and deformation to cease to be linear and, therefore, no longer follow Hooke's law [6]. This can be seen during the tensile test when analyzing the stress vs. deformation graph.

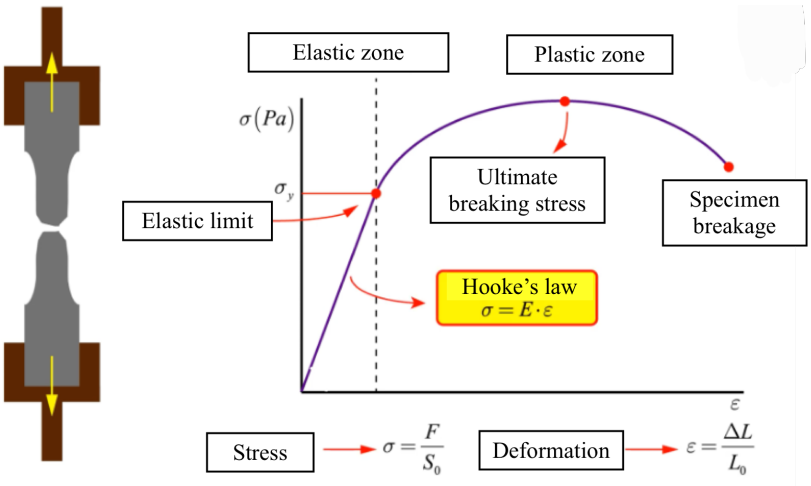

Figure 16 Stress Vs. Deformation (Source: [6])

During a bending test for a ductile material, when the elastic zone passes, the stress distribution loses the linear relationship, the extreme fibers begin to plasticize while the central fibers are still in the elastic regime. Making the equations only useful for strictly elastic conditions.

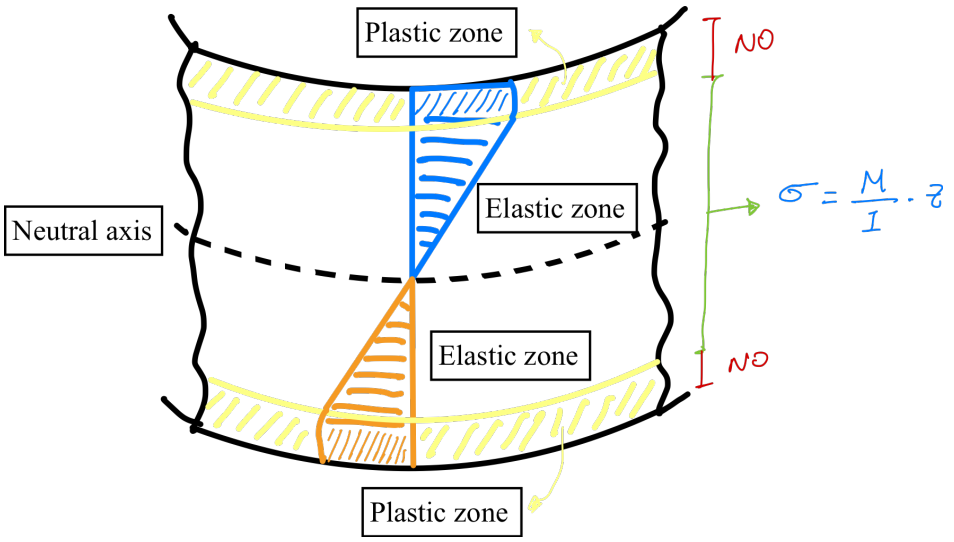

Figure 17 Plastic and elastic zone distribution.

During the bending test, the machine records the applied load and the punch stroke, which corresponds to the deflection in the specimen. A graph is obtained where the straight elastic zone is distinguished, followed by the appearance of the plastic regime. The force value that marks the beginning of plasticization is the maximum load in the elastic regime, so this will be used to calculate the bending yield strength of the material. This limit indicates the maximum axial stress that the material withstands when bending before starting the plastic regime.

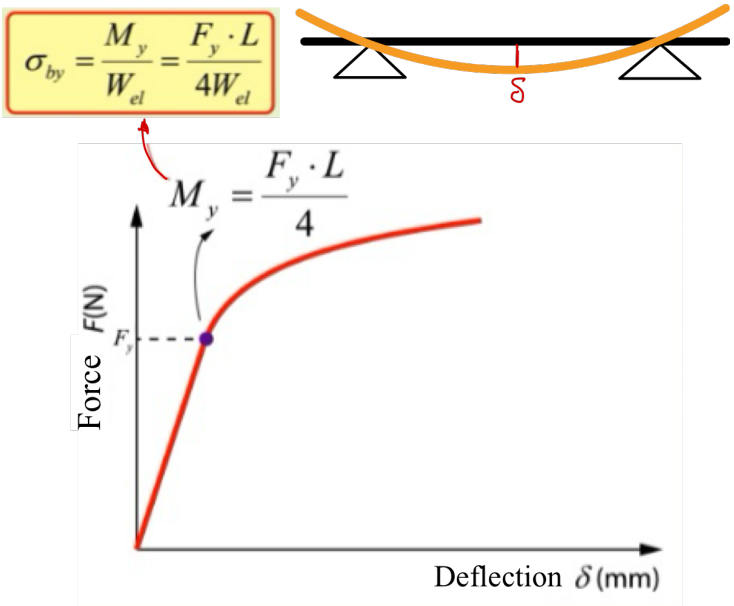

Figure 18 Deflection Vs. Force diagram (Source: [6])

The yield strength obtained in the tensile test should coincide with the one measured at bending, however, in practice the yield strength at bending is usually approximately 10% higher, since identifying the starting point of plasticization is difficult because it only starts in extreme fibers, being a very slight curvature in the graph [6].

$$\sigma_{by} > \sigma_y$$

It is possible to obtain the elastic modulus of the material under bending, from the calculation of beams, relating the deflection in the beam with the force applied, the length between supports, the elastic modulus and the moment of inertia [12]. There are only deflections in the elastic zone, where the equation is valid, and with this the value of the flexural elastic modulus can be calculated.

$$\delta = \frac{F * L^3}{48 * E * I}$$

$$E = \frac{F * L^3}{48 * \delta * I} \tag{17}$$

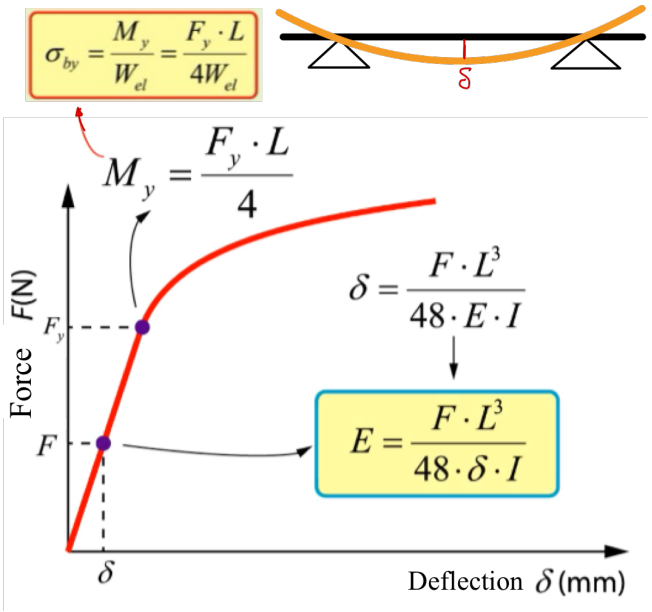

Figure 19 Elastic modulus of the material under bending. (Source: [6])

2.2.2 Material Conditions and Bending Test Results

The bending test is very useful for analysing brittle materials, because the tensile test is usually not very favourable for the propellants of these materials, thus making it difficult to obtain reliable results. The jaws may fracture the specimen head due to excessive tightening, or the specimens may be placed misaligned with respect to the test axis, and this generates an anticipated breakage, problems that do not occur in the bending test [8].

For a brittle material, the specimen will break without reaching a large deformation, obtaining a much shorter curve, as shown in the Figure 20 [10]. The

fracture arrives very soon after overcoming the elastic zone and, although the linear relationship between stresses and deformations is no longer maintained, as the curvature that is recorded is so small, the flexural fracture stress can be calculated for the maximum force reached, assuming a minimum error [9]. In the same way, the maximum deflection to fracture is indicated, based on a length *L* between supports.

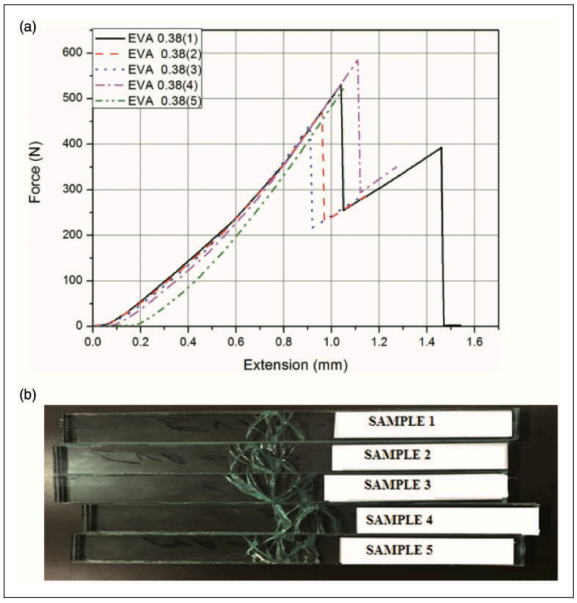

Figure 20 Force–extension curve of glass samples (Source: [10]).

Normally the specimen will break through the traction zone. If there is a crack in the material, it will begin to open and it will be in the crack where the fracture begins. On the other hand, if the cracks are in the compression zone, they are not dangerous, since they close during the test and do not initiate the failure, so they tend to be ignored [8]. It is for this reason that fragile materials resist compressions much better than tensile stresses.

So, if the position of the crack will cause the failure to be generated in that section. If there is a crack in the specimen in a section other than the central one, the failure will occur for a different bending moment and stress value than the one calculated, since bending test calculations are generally performed for the central position where the load is applied to the specimen. In that case, the test will fail since the position of a crack is uncontrollable and would give us wrong results.

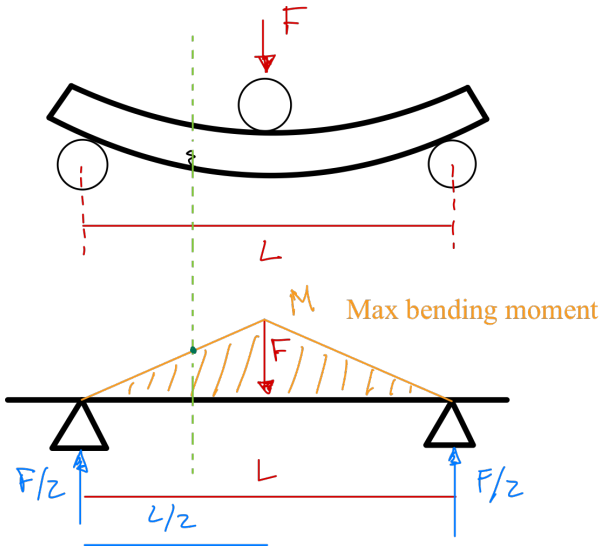

Figure 21 Diagram of forces and momentum with a crack on the beam

On the other hand, certain experiments will require the presence of a crack to be successful, so it is often necessary to perform cracks in the specimen in order to induce failure and study the propagation of the crack at a known and predictable point [11]. This type of study allows us to evaluate the behavior of a crack and its propagation under controlled conditions, such as studying the propagation of cracks in a given material or studying the behavior of a material under work cycles [11].

a) Test specimen with the pre-crack

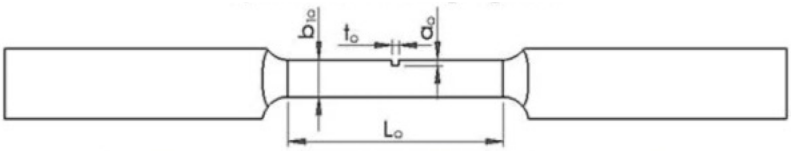

b) Dimensions in the section where the pre-crack was made

Figure 22 Pre-cracked specimen (Source: [11]).

If the effect of the crack in the specimen is to be avoided and the bending test can be performed, the bending test could be performed at four-points bend configuration. The load is now applied by two loads symmetrically, resulting in a constant bending moment diagram distribution in the central area, eliminating the possibility of crack position affecting the test [8][9]. In addition, the four-point bend configuration is closer to pure bending than the three-point bend configuration, because there will be no shear stress in the central area where the force was applied [8].

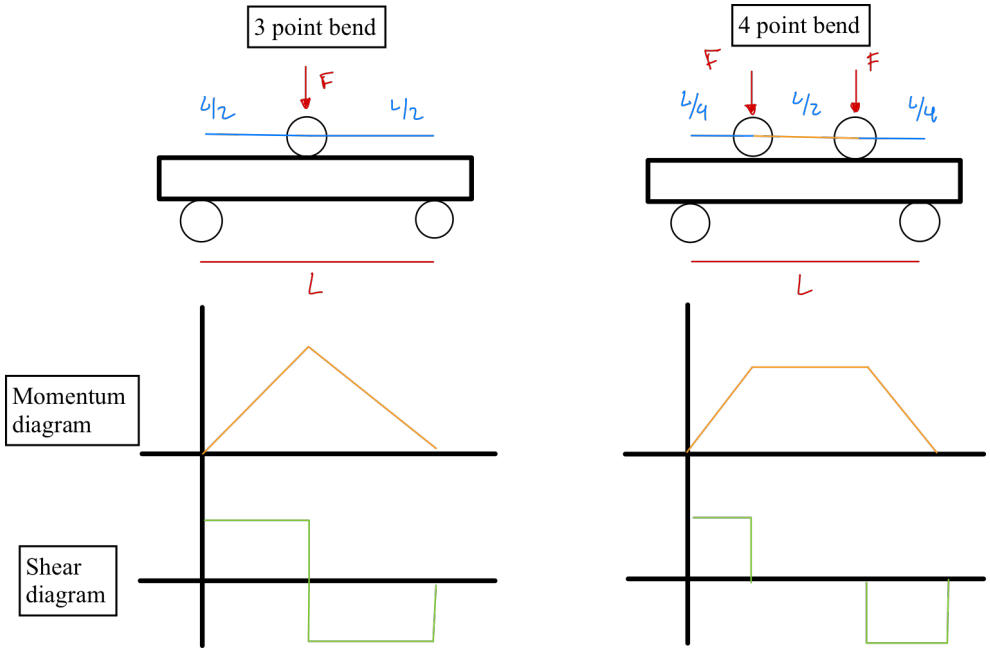

Figure 23 3-point bend Vs. 4-point bend diagrams

When it comes to ductile materials, it is not necessary to consider a tensile stress during the bending test, because usually the material does not break, but rather slips between the supports due to deformation, as can be seen in the image.

Figure 24 Bending test in a ductile material (Source: [7])

In the same way, with ductile materials it is not possible to obtain a stress-strain curve such as those obtained with a tensile test, because the equations are not applicable in the entire curve, due to the presence of an elastic zone, which would result in stresses that do not represent what happens to the material in reality [6].

2.3 Test Machine

Universal testing machines test the mechanical properties of materials, components and products. They can be powered by electromechanical or hydraulic means for different types of tests, such as tensile, compression, bending, peeling or tearing [16]. As the sample is bent or flexed, it is subjected to a combination of tension, compression, and shear forces. That's why bending tests are used to evaluate the reaction of materials to realistic load situations [15].

Low-force tests are generally performed on electromechanical machines, while higher-force tests are used on floor model machines [15]. Universal testing machines are used to evaluate materials such as polymers, metals, elastomers and composites [16].

2.3.1 Common Materials for Bending Tests

Polymers are tested with 3-point grips. The deflection of the specimen is measured by the position of the crosshead. It is generally used to measure the flexural strength and the flexural modulus.

Wood and composites are tested with 4-point grips. According to standards, a deflectometer is required to measure the deviation of the sample in the center of the support span. Flexural strength and flexural modulus are usually measured.

Fragile materials such as glass and ceramics can be tested with a 3-point grip to calculate the Flexural Strength using the modulus of rupture (MOR), stiffness cannot be calculated with this configuration. 4-point grips can also be employed but the alignment of the supports becomes crucial, and the load configuration becomes critical to change [15].

All processes, obtaining samples and performing tests are regulated by standards such as ISO, ASTM, etc., all depending on the material to be tested and the result to be obtained.

Some of the main standards for bending tests:

- ASTM D790: Standard Test Methods for Flexural Properties of Unreinforced and Reinforced Plastics and Electrical Insulating Materials
- ISO 178: Plastics - Determination of flexural properties
- EN 408: Timber, sawn timber and glulam structures for structural use, determination of certain physical and mechanical properties
- ISO 7438: Metallic Materials-Bend test
- ASTM E290: Standard test methods for bend testing of material for ductility.

3 Overview the Possibilities of Optical Stress Field Measurement and Evaluation

The possibility of measuring stress fields in a non-invasive way has favored the study of these fields since they allow them to be analyzed completely without interference, that is, unlike using strain gauges where we can measure punctually in a specific section of the material, optical methods allow analyzing the deformations and stresses and how these are distributed throughout the entire specimen. which is especially useful in projects like this where it is necessary to analyze the tension gradients along the entire surface, both in length and thickness, of the specimens.

The great advantage of these techniques is that the analysis of the components are the closest to reality, without the need for simplified modelling of the geometry, material, loads or constraints that would be involved in carrying out other types of experimental tests, such as tests by means of extensometry, therefore their results are more accurate to the real situation of the component. however, they entail the need to design a first prototype with which it can be tested.

Among all the optical techniques available that can be used to measure deformations, displacements, stresses, etc., some stand out due to their advantages such as studying materials in a non-destructive way and without contact with the specimens. Considering the objective of this study, which is the design of a bending testing machine with a 3-point Jig, several alternatives were taken into consideration to be able to measure stress optically, which we will analyze their pros and cons below.

3.1 Photoelasticity

Photoelasticity is an optical measurement technique that serves to evaluate the stresses to which a birefringent part, generally made of transparent acrylic plastic, or some translucent material is subjected when subjected to mechanical stresses [19]. This technique consists of placing two crossed polarizers in front of a uniform light source. By observing the color pattern in the material in the middle of the polarizers, you can evaluate the points where it is subjected to greater stresses. The assembly is observed through polarized filters which show the information of stresses in the strips [21].

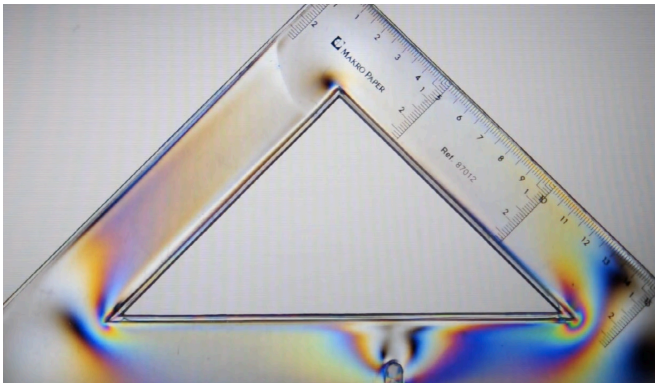

Figure 25 Homemade polarimetry in an acrylic square (Source: [25])

As can be seen in the figure, the more colors are present in the same area, the greater the stresses present and therefore the more likely it will be to break at that point.

The phenomenon is based on the polarization of light and the use of a birefringent material.

3.1.1 Physical and Optical Principles of Photoelasticity

As mentioned, in order to perform a photoelasticity test, it is required that the part to be studied be made of a translucent material or that it be previously prepared with a photoelastic coating, generally some type of polarizing film, which allows the analysis of real components of practically any size and shape under the real service load conditions [26].

At a point in a luminous ray, we can schematize natural light, both white and monochromatic, as an infinity of vectors perpendicular to the ray, whose modulus varies sinusoidally over time. If the light is monochromatic, all waves will have the same wavelength in all planes. If, on the other hand, it is white light, waves with different wavelengths will also be superimposed in all planes [26].

If a rectilinear polarizing filter is placed, it will only allow the vibrations that occur in its preferred direction of polarization to pass through, gradually extinguishing the others, to the point of canceling out those that are perpendicular [26]. At the exit of the filter, the light is polarized. If the filter is rotated around the axis defined by the light ray, it rotates the direction of polarization of the light [26].

If a second polarizing filter, called an analyzer, is now placed on the beam that has come out of the first filter (polarizing filter) so that both have parallel polarization directions, the light ray will be able to pass through them [26]. However, if one of them is rotated, in this case the second one with respect to the other, until both are perpendicular, what will occur is the extinction of the ray, this means that if we turn the second polarizing filter enough we will be able to see the entire spectrum of light on our sample and therefore all the stresses to which it is subjected.

The waves from the light source passing through the filters cause the light to break down into its components, and when it reaches the birefringent material it makes one wave slower than another due to the deformation of the internal structure of the material, and when passing through the recompositing filter again this new wave will not have the same orientation as the wave before passing through the sample material [26]. This new wave will not be extinguished when it passes through the filter again and will therefore be visible in the form of isochromatic stripes as can be seen in the figure [26].

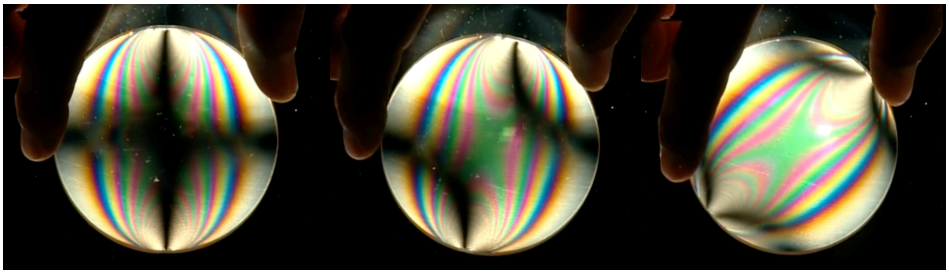

Figure 26 Isochromatic lines present during the photoelasticity test (Source: [26])

As can be seen in the figure, as the orientation of the filter is changed, different fields can be observed through the material studied.

3.1.2 How the Circular Polariscope Works

This type of photoelastic testing is usually carried out on a machine known as a circular polariscope, the general configuration of which can be seen in the figure below.

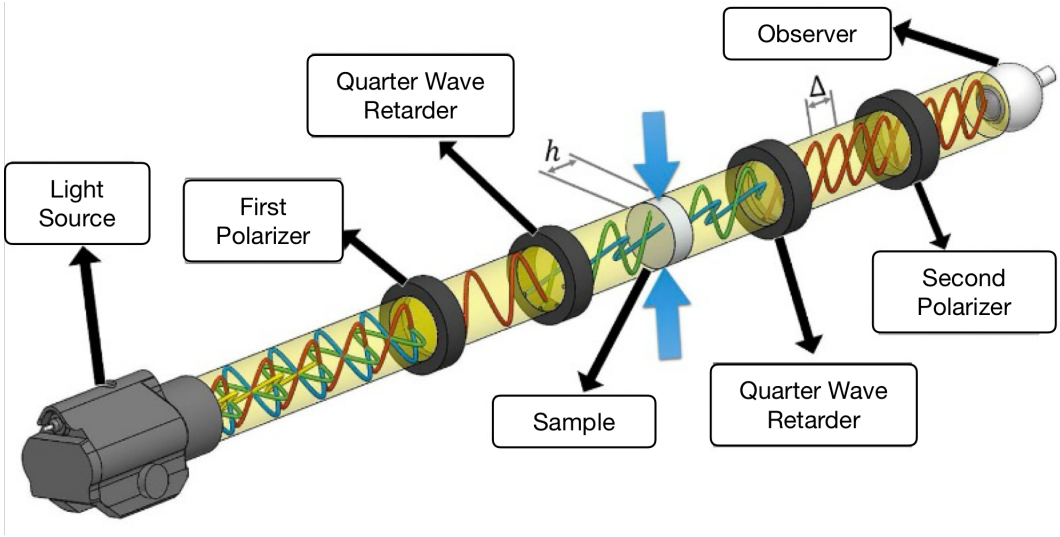

Figure 27 Diagram of operation of a circular polariscope (Source: [27]).

As you can see in the figure, the entire system starts with a light source, usually a white LED light, which emits a uniform beam of light onto the specimen. The beam of light passes through a first polarizing lens, which linearly polarizes the incoming natural light, causing the light to vibrate in a single, defined direction.

The next filter is a quarter-wave retarder, usually aligned at 45° to the direction of polarization, which will transform the polarized linear light into a circular one which allows the test result to be non-dependent on the orientation of the specimen [27].

The circular polarized beam of light will pass through the translucent specimen of a birefringent material which breaks down the light and induces a wave mismatch in the light causing it to travel at different speeds through the specimen [27]. This mismatch is directly related to the state of the stress field within the specimen [27].

The light beam will then pass through a second quarter-wave retarder which will again transform the polarization state of the light making it possible for it to be processed and analyzed.

Finally, the resulting beam of light will pass through a second polarizing lens, usually aligned at 90° with respect to the first, making the stress fields visible over the sample. This is thanks to the fact that when the specimen presents stress in its geometry, the presence or absence of these stresses causes the resulting light to be dark, so that the mismatch resulting from the birefringence of the light will indicate the presence or not of stresses on the specimen [27].

At the end of the entire system, the circular polariscope allows the forces to manifest themselves on the study material through light intensity showing a pattern of colored lines which represent the distribution of internal stresses and deformations on the studied specimen, which can later be measured and analyzed.

The contrast obtained in its results is good, in addition to the fact that it allows us to observe the entire stress field making it ideal for beam models.

3.1.3 Advantages, Disadvantages and Experimental Conditions

As can be seen in the following image, the standard configuration to perform photoelasticity tests is very complex and sensitive, because it requires very specific and complex optical systems as well as special equipment such as lasers and controlled environments in order to maintain critical alignments and avoid vibrations and noise that can alter the results.

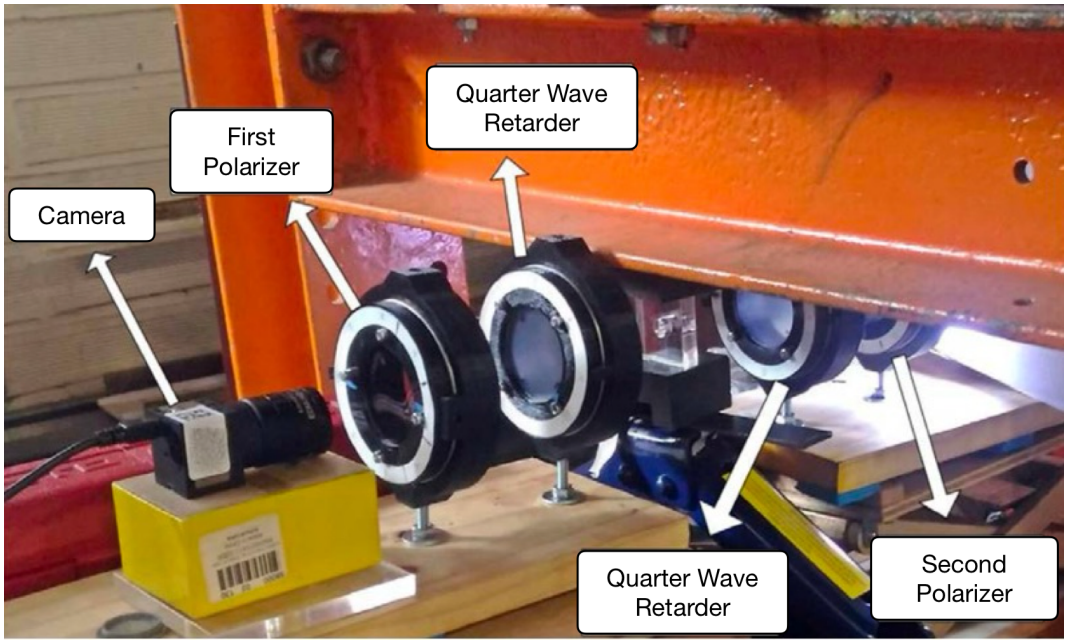

Figure 28 Optical Mounting of Photoelasticity Test (Source: [27])

In the same way, it is worth emphasizing the need for special materials in the specimens, which make them very impractical for tests on common engineering materials such as steels or polymers.

However, the System is not standardized in its application because each analysis requires its own specific set of steps and set up in order to describe the distribution of efforts, for example, in the image shown the specimen was placed on a hydraulic jack and not just a universal testing machine; in addition, with complex geometries the reading of the stripes becomes complex and we will require special software or computers with high computing power to analyze the data.

3.2 Electronic Speckle Pattern Interferometry (ESPI)

Electronic speckle pattern interferometry or ESPI It is a non-destructive and non-invasive optical measurement technique used to measure the displacement, deformation and the cracks displacements upon loadings into a specimen with extremely high sensitivity to the nanometer level [30]. Its operation is based on using the interference properties of the light of a laser applied to the specimen to be studied to obtain measurable results on it [28].

3.2.1 Physical and Optical Principles of Electronic Speckle Pattern Interferometry

As mentioned, the operation of the ESPI is based on interferometric principles, in a simple way, a laser sends a beam of light on the specimen which will reflect on

the surface of the specimen creating a random pattern called "speckle" which represent the deformations present on the surface of the specimen [29].

When the specimen is illuminated by the laser applied with coherent light, it will obtain a granular appearance, the speckle, caused by the random interference of light reflected from various points on the rough surface of the specimen [22].

A camera will capture these resulting images and compare the phases of light with the initial images thus obtaining an interference pattern [29], this is done by means of a technique of subtraction of intensities comparing the light pattern before and after applying the load on the specimen [22]. These resulting patterns require special interpretation and post processing making the data analysis of this assay complex.

As can be seen in the figure below, the result of the electronic speckle pattern interferometry study will be an image full of light and dark stripes, called interferograms, which represents places of equal phase difference [22], this phase difference is related to the optical path, and how this will vary, introduced by the movement of the surface of the specimen [22]. To put it simply, each strip present is a phase difference that represents a specific amount of displacement of the specimen surface. These variations can be so sensitive to the range that nanometer variations present in the test can be measured during the test.

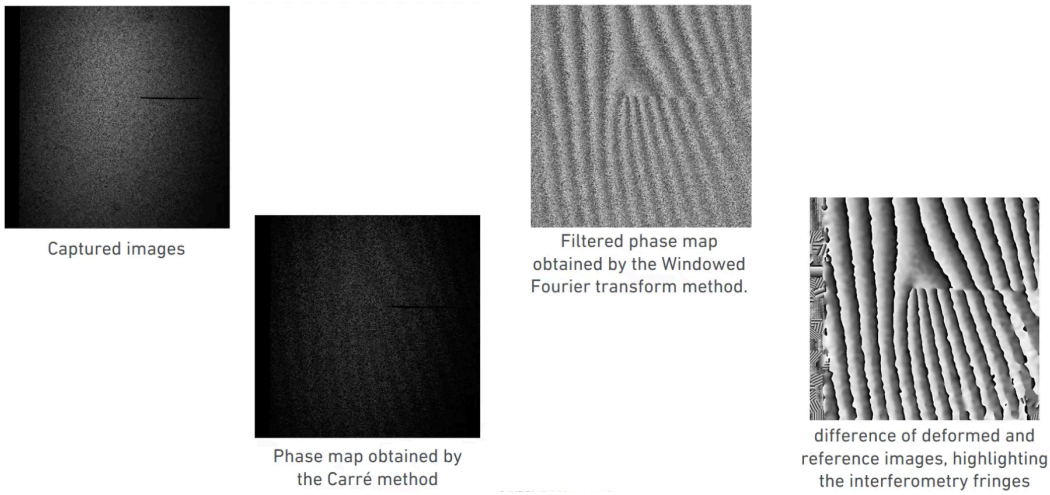

Figure 29 Image acquisition processing on electronic speckle pattern interferometry (Source: [30])

Similarly, if the specimen has defects, such as cracks or pores, these will be seen as anomalies or distortions in the stripe pattern, thus allowing the identification of the failures present in the specimen [22]. As can be seen in the figure, the specimen studied had a crack on its surface and this is represented in the final image as a line crossing the image which alters the pattern of lines.

Depending on the test setup, the orientation of the lasers, and the arrangement of the mirrors, an electron speckle interferometry test can detect both in-plane (transverse) and out-of-plane (toward the camera) displacements, as well as their strain gradients, that is, their derivatives [22].

3.2.2 Standard Set-up for Electronic Speckle Pattern Interferometry

The image below shows a standard set-up of an electronic speckle pattern interferometry test, which basically consists of a laser which will emit a coherent and monochromatic beam of light, usually white [31]. Followed by a beam splitter which will divide the light beam in two: the light beam that will go directly to the specimen and the reference beam, as the two beams of light come from the same source, it allows us to maintain the same initial phase for both beams of light before interacting with the specimen [22].

Once the light beam has been divided, one of these will pass through a convergence lens, which will be responsible for converting the divergent light rays into parallel rays, with which we will obtain a constant and uniform illumination on the specimen [31]. The second beam of light will pass through an expanded laser beam which will be responsible for illuminating the entire area of interest or ROI of the specimen thus allowing a complete measurement of the stress field [31].

Finally, the resulting image is observed through special cameras which will record the speckle pattern and the variations in light intensity, converting the resulting optical image into digital signals that the computer can display and process [31].

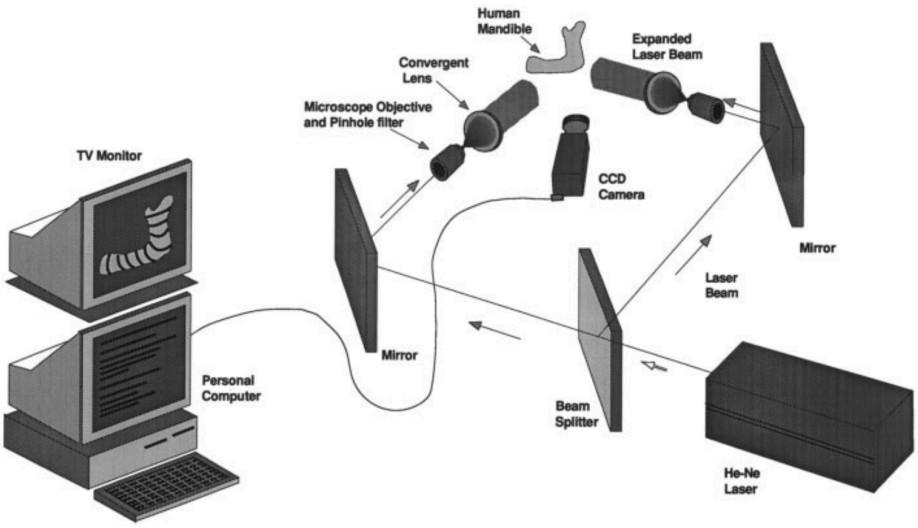

Figure 30 Set up for electronic speckle pattern interferometry (Source: [31])

3.2.3 Advantages, Disadvantages and Experimental Conditions

As can be seen in the figure below, this shows a real assembly in the laboratory for an electronic speckle pattern interferometry test, as you can see this carries a great complexity in its assembly and in its working conditions, because it requires very delicate optical configurations when using special lasers and splitters for the

light beam, and also, because it must maintain a precise alignment that does not alter the expected results.

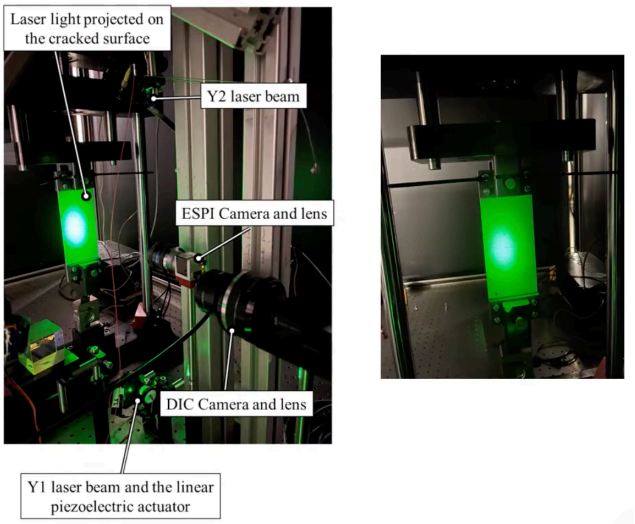

Figure 31 Laboratory set up for ESPI (Source: [30])

Controlled environmental conditions such as having an anti-vibration table, environmental isolation, thermal stability, special cameras, etc., are required, all in order to prevent any external vibration from affecting the measurement and therefore giving us noise in the interferometric signal [31].

This interference gives information about displacement or deformations on the surface. It is very sensitive having good response and high sensitivity to the smallest defects being able to detect in the range of micrometers.

However, it is a very sensitive system to vibrations and environmental conditions, in the same way, preparing the test is very complex as well as its data processing making an electronic speckle pattern interferometry test more viable as an optical laboratory test than in a functional and practical testing machine which is the purpose of our study, which presents a mobile loading system during the test and therefore invalidating the measurements with this technique.

3.3 Digital Image Correlation (DIC)

DIC is a testing and analysis method that relies on images from digital cameras to extract 2D and 3D full field data on the test object. The information is captured from a random pattern of points over the specimen called speckle pattern, extracting the geometry of the tested area as well as the displacement, could be 2D and 3D depending on the camera system used, on all the points with a spatial resolution equivalent to that of a finite element model [35].

It is a technique that allows deformations to be measured visually and in real time. This technique takes a sequence of images to the specimen while the test is being performed, which has a random pattern imprinted, the pattern in the specimen

will generate variations in intensity that allow identifying regions within the image that will allow its movement to be tracked with dedicated software. And at the time of analyzing the images, a specialized software will track the pixels based on the points of the initial pattern in the sample to see in sequence with each frame how these points were displaced in relation to their previous frame or in front of a reference image.

Image analysis using a single camera is limited to 2D deformation analysis, however, by placing a multi camera system it can be tracked over the entire surface thus obtaining a 3D result of the deformation in the specimen [35]. Analysis with a single camera or 2D DIC is generally used for flat surfaces, while 3D DIC or also called Stereo DIC, by using two cameras with a certain angle, allows to capture three dimensional displacements and deformations and compensate for out of plane movements [24]. This offers the possibility to precisely capture local behaviors, derived strain, velocities, accelerations, stresses, curvatures, etc., with good lighting, a well done speckle pattern on the specimen and cameras. DIC delivers extremely accurate full field experimental characterization and identification of material properties, as well as a quantitative validation of structural models.

For materials testing, you can use DIC to determine and identify mechanical properties by measuring the static and quasi-static loading of material samples on dedicated testing machines [35]. For our case study, in which we need to measure the stress field of a specimen during a bending test, this approach is advantageous because it would allow us to continuously obtain information across the entire surface of the specimen, where significant strain gradients exist throughout its surface [36]. For structural testing, DIC can be used to perform static and transient testing for components and systems, in the same way, measure full field strain field on their load to reliably validate numerical models [35]. Finally, for structural dynamics testing, DIC can be used for conduct full field contactless modal and vibration testing and analysis with cameras or by combining cameras with traditional sensing techniques, in a hybrid technique that would allow stress to be measured in the entire field and with gauges to be able to measure in very specific areas.

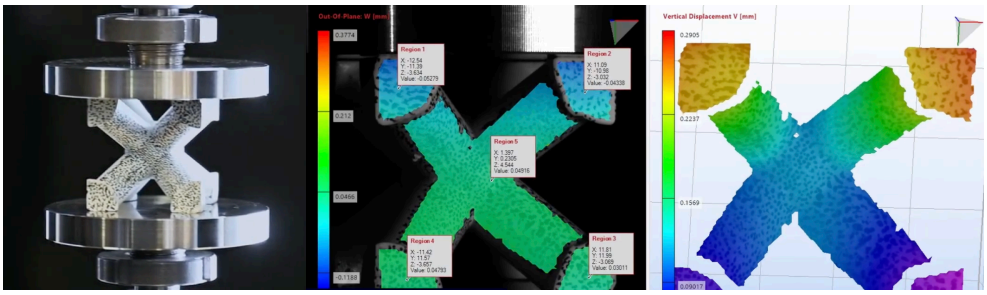

Figure 32 Material testing using DIC technique (Source: [35])

The position of the cameras and the light greatly influence its result, making sure we get as much information as possible from the images by making it easier for the software to track more points of the pattern and giving us more surface information.

3.3.1 Surface Preparation for Digital Image Correlation

As previously mentioned, the operation of DIC and a good quality in its results is based on the following of a speckle pattern on the specimen in a sequence of images, so it is essential that the quality of the image and this pattern is well printed on the specimen´s surface.

To ensure this, the specimen must have some prior preparation, starting from a deep cleaning of the surface [23]. A quick cleaning with a wipe with alcohol is a good idea before any painting. Acetone may be required for heavier deposits on metals. Some materials may require roughing of the surface using sandpaper to improve paint adhesion [37].

Depending on the surface of the object, it is often necessary to apply a base coat to the surface prior to speckling, A white background is usually applied, and the speckle pattern is black to obtain a good contrast in the image [24]. Usually, for most speckling methods, the surface of the specimen is coated white with several very light coats of matte spray paint. Satin or gloss paint can cause specular reflections, especially under intense lighting, and should be avoided [37]. It is recommended to apply many coats very lightly, as heavy coats may lead to drips forming, which change the shape of the surface [37].

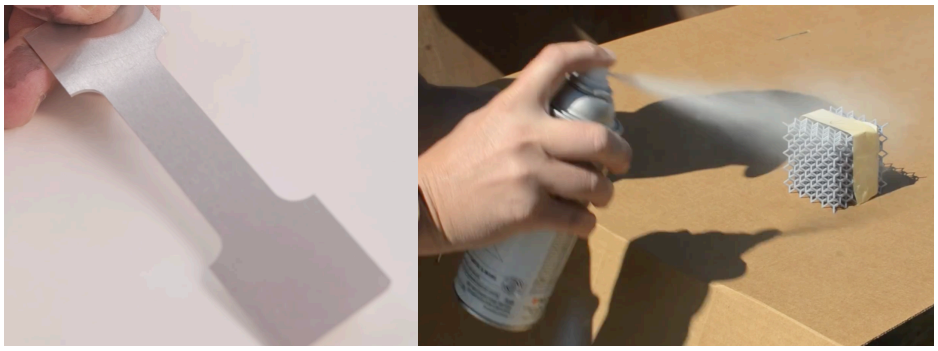

Figure 33 Surface preparation before applying a speckle pattern (Source: [37])

Once the surface is perfectly clean and with the white paint base applied, it is prudent to wait until the base coat is completely dry before applying speckles. If the base coat is still wet, the speckles and base coat can blend, which reduces contrast and may result in the pattern appearing blurred in the images [37].

3.3.2 Speckle Pattern for Digital Image Correlation

Once the clean surface is ready and, if necessary, with a paint base that contrasts with the speckle pattern that is going to be applied, we will proceed to impregnate the specimen with a random pattern of dots that will be used by the image analysis software to study the stress field. Using an optimal speckle pattern is one of the most important factors in reducing measurement noise and improving overall DIC results.

In DIC, a mesh of small subsets of the image are tracked as the specimen moves and deforms. To perform this tracking, the subsets are shifted until the pattern in

the deformed image matches the reference image as closely as possible. This match is calculated by the total difference in gray levels at each pixel within the subset.

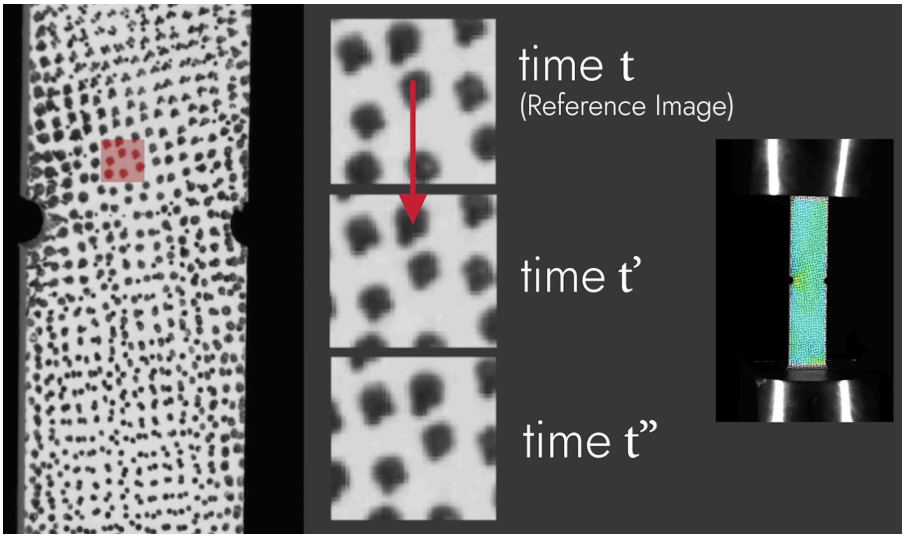

Figure 34 Deformation of a speckle pattern during a mechanical test (Source: [37])

Generally, the speckle pattern needs to deform with a sample and not reinforce it, and it must hold up to testing conditions like temperature, moisture, and acceleration.

To provide quality tracking information, DIC speckle patterns should feature the following characteristics:

- High contrast: The pattern should feature either dark black dots on a bright white background or bright white dots on a dark black background [24]. The greater the contrast of the speckle pattern on the specimen, the better the image tracking and therefore the better results.

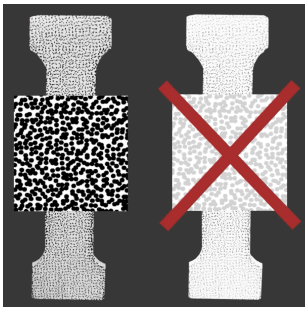

Figure 35 High contrast of the speckle pattern on the specimen (Source: [37])

- At least 50% coverage: A correct pattern has around equal amounts of white and black on the surface and with an approximate feature size of 3 to 5 pixels [24]. For example, if the speckles are five pixels in size, they should be approximately five pixels apart from one another.

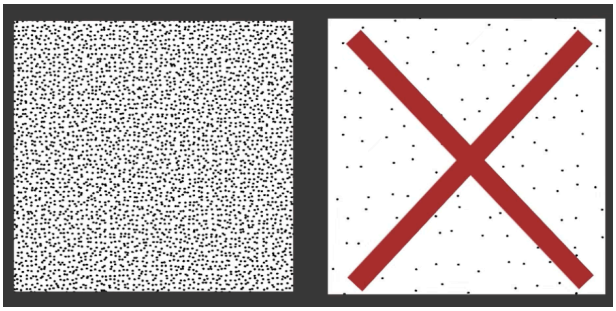

Figure 36 Correct distribution of speckle patterns on the specimen surface (Source: [37])

- Consistent speckle sizes: Speckles should be 3 to 5 pixels in size to optimize the spatial resolution [24], however, the most important thing in the speckle pattern is that the speckles must be consistent in size and not too small. Less than three pixels in size is too small and can cause aliased results.

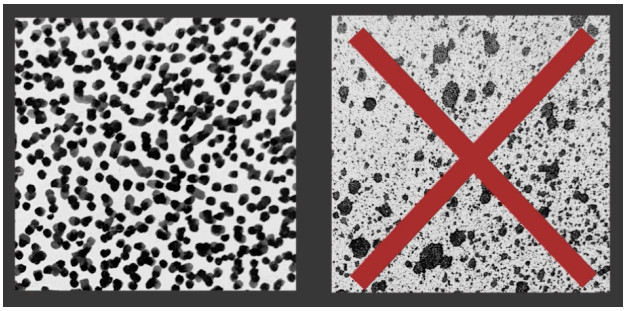

Figure 37 Correct size of speckle patterns on the specimen surface (Source: [37])

- Isotropic and stochastic: The speckle pattern should not exhibit a bias in any particular orientation, and it should be random [37]. A not random pattern is difficult to achieve a pattern regular enough to cause false matching. In the same way, it is necessary to achieve through the technique we use to apply the speckle pattern on the specimen that the dots are uniform, and we do not obtain lines or smudges on the surface of the specimen.

Figure 38 Correct form of speckle patterns on the specimen surface (Source: [37])

If the pattern has speckles that are too large or if it is too sparse, we find that certain subsets may be entirely on a region of black or a region of white.

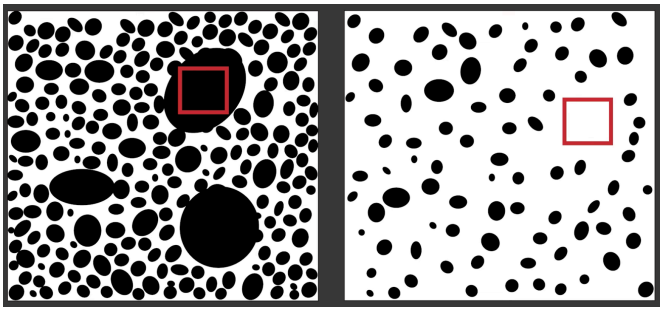

Figure 39 Region of interest in an area with a bad speckle pattern (Source: [37])

This generate a bad correlation because everywhere in that region is an exact match. To avoid this, we can increase the subset size, but this is done at the cost of spatial resolution. In the same way, if the pattern is too small, the resolution of the camera may not be enough to accurately represent the specimen.

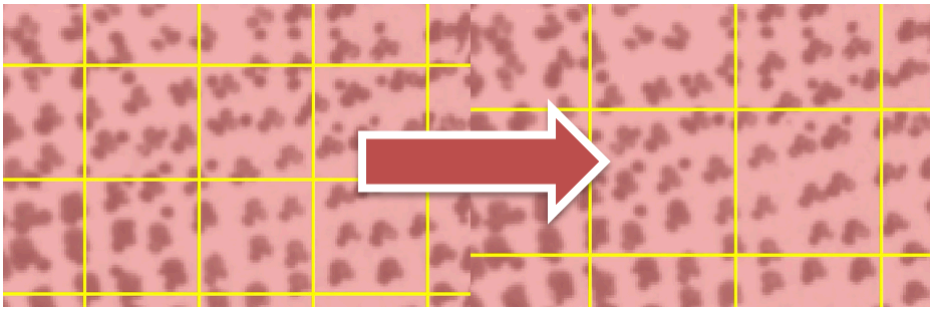

Figure 40 Resizing the subset in the same region of interest (Source: [37])

To prevent the speckle pattern from being blurred or of poor quality, we can play with the resolution of the camera and the field of view to obtain better quality in the visualization and tracking of the speckle pattern on the specimen in the images taken during the test.

It is worth emphasizing that the quality of the speckle pattern has a direct result on the effectiveness of the test. A good pattern will allow the correlation to be made with high quality and produce low noise.

3.3.3 Advantages and Disadvantages of Digital Image Correlation

One of the advantages of this technique is that there is no interference from the system on the specimen, making it non-contact and non-invasive. This is very useful for microscale measurements where specimens are fragile [23]. In the same way, this technique is widely used for biological materials or microscale samples where placing a physical sensor would alter the behavior of the material or would be impossible due to its size or material properties [32].

As previously mentioned, the digital image correlation technique allows a complete field study allowing to study the entire surface of the specimen and obtain continuous deformation results of the entire surface, thus allowing to identify hot

spots where there are cracks, defects in the material, pores, and other spatial gradients that sensors or traditional techniques could not easily identify [32].

Unlike other techniques such as photoelasticity, digital image correlation allows the study of various materials and scales, as they are not dependent on a specific material to function as in the case of photoelasticity where only translucent materials could be worked with, thus allowing a wide range of materials that could be analyzed by DIC as metals, concrete, polymers, woods, etc. in the same way being able to work with more complex geometries and varied sizes, both at nanometric and metric scales, such as the study of a standard specimen of 12 cm long to a structure or large piece such as a bridge or an airplane wing, this only depending on the speckle pattern that we apply to the surface and the camera with which we obtain the images [33].

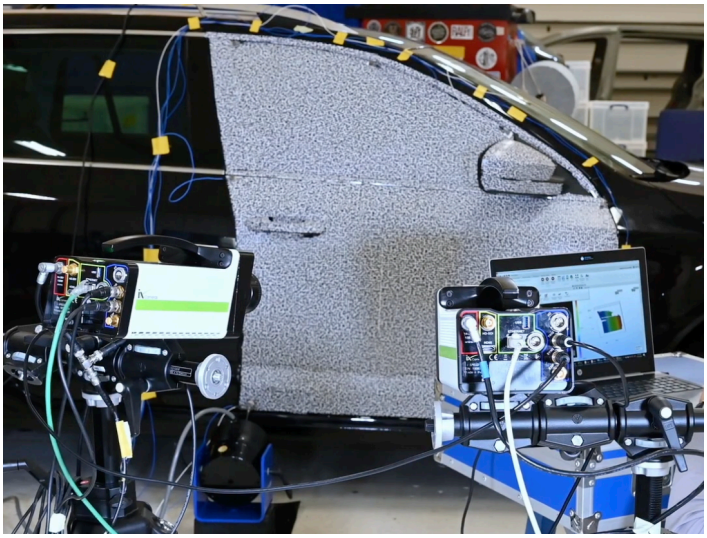

Figure 41 DIC test to an entire car door (Source: [35])

Like other techniques reviewed in this study, the DIC can also be combined with other experimental testing methods such as sensors or finite element validation (FEA) in order to compare and validate results [32]. Comparing the study of a stress field using DIC against the traditional use of strain gauges, it is worth mentioning that the DIC obtains results globally over the entire surface of the specimen while the gauges only obtain deformation results on the point where they are placed, it is also worth mentioning that when using gauges or other types of sensors on the specimen these may present assembly errors which can generate stress concentrators or that the sensor in turn moves or slides on the surface [23].

Similarly, the DIC is the only way to measure stress fields in micro sized samples where it is impossible to place sensors or traditional strain gauges due to their size, and these are simply very complex or impossible to attach [38]. In the same way, it is the only way to be able to study more sensitive materials such as film, which is highly affected when in contact with traditional sensors [38].

The process is standardized so it is easy to implement following guides on how to carry out the experimentation, from how to prepare the pattern, to how to track

the pixels correctly with software [24]. In the same way, combined with a bending test as is the objective of this study, the DIC allows monitoring displacements and cracks on the surface in a better way and allows measuring the toughness of the fracture in a more dynamic way than traditional methods such as sensors and strain gauges [19], making it possible for the results of bending tests with digital image correlation and those obtained by discrete sensors to be comparable and validable with each other [34].

Field study using digital image correlation promises to be an effective and simple study for almost any type of material and size required. However, the DIC still presents challenges such as the dependence on a good speckle pattern on the surface of the specimen, good cameras that allow you to see the pattern on the surface in a good way, which can become a significant expense depending on the scale of the study you want to carry out, as well as in case two cameras are required for a 3D DIC studio.

Speaking of Image Quality, it is worth mentioning the subset size in the region of interest of the image, which poorly configured can give us noise in the studio and in turn alter the deformation gradient [24].

3.3.4 Set-up for Digital Image Correlation and Image Acquisition

Once we have the specimens ready with the speckle pattern on their surface we can start obtaining images by digital image correlation. Unlike other optical field analysis techniques such as photoelasticity or electronic speckle pattern interferometry, the set-up to be able to perform digital image correlation is quite simple and does not require complex materials or configurations.

As shown in the figure below, the basic setup for performing mechanical tests and obtaining results using 2D DIC on a flat surface consists of a light source, usually white light, that provides good illumination of the speckle pattern on the specimen's surface, thereby creating good contrast between the black and white areas of the pattern to enable tracking of the points in the images. Similarly, a camera must be pointed at the specimen at all times during the test, allowing us to obtain an initial reference image and a final image showing the deformed specimen.

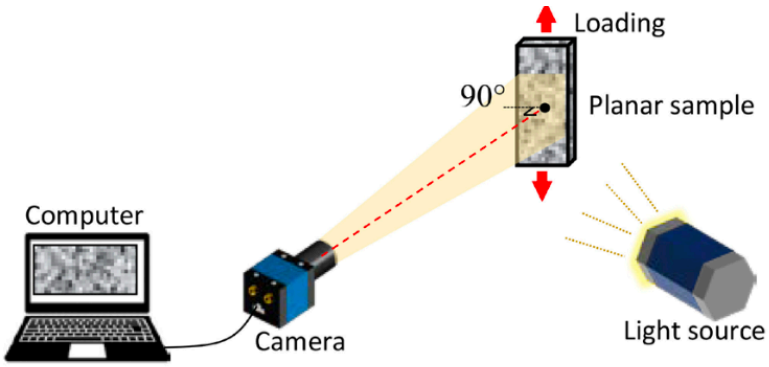

Figure 42 Set-up standard for 2D digital image correlation (Source: [36])

To review the image acquisition process for digital image correlation, we begin by setting up our equipment according to the requirements of our experiment. In our case, this involves a setup for testing on flat surfaces, that is a 2D DIC, for which we will need a camera to capture the images, a white light source, and a specimen that has been prepared and is ready for testing, with a speckle pattern on its surface.

Once we have the set up ready, we will proceed with the configuration and calibration of the system, where we will mount the cameras in a stable and fixed way pointing at the specimen but first using geometries known as patterns to be able to calibrate the cameras, correcting the focus and distortions of the lens, as well as measuring the distance between the camera and the specimen [24].

Next, we will proceed to obey the reference image, which is nothing more than an image of the specimen in its initial condition before being subjected to any type of deformation, in our specific case before performing the bending test on it [24].

Once we have the reference image, we will proceed to start the mechanical testing equipment and we will carry out the test, this in turn the camera began to record or obtain a sequence of images of the process that we will later use to perform digital image correlation. Once the test to the last image is finished, whether it is the last image before the rupture of the specimen or the last image before the maximum deformation of the material, we will consider it the deformed image. Which at the time of image analysis we will compare with the reference image to see how it was deformed [24].

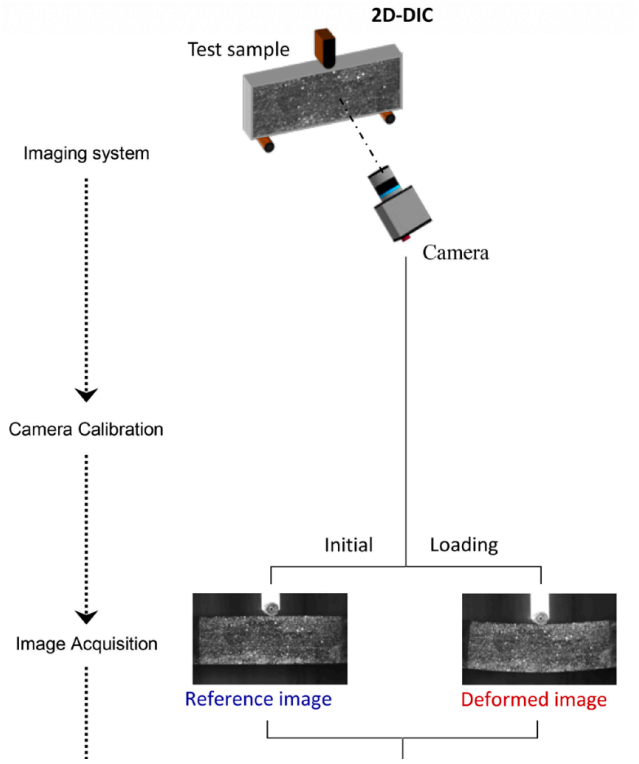

Figure 43 Image acquisition using digital image correlation (Source: [36])

Now talking about image processing and obtaining results, the images obtained we could pass them through a kind of image editor where we could improve the quality of these or in turn perform a threshold with the aim of converting the images obtained to binary images, that is, in black and white, with which the objects of interest are separated, in this case the speckle pattern on the surface of the specimen, with the other elements of the background thus being able to follow the pattern on the surface in a better way [24].

Once we have the images ready, what we proceed to do is to use some point tracking software or some specialized software for digital image correlation (The calculations and the model in which the points on the speckle pattern are tracked are outside the field of this study so they will not be mentioned and existing tools for this study will be used) we will proceed to select the region of interest, which will be the surface of the specimen, and the software will be in charge of creating the subsets, thus calculating the displacement and deformation fields using optimization algorithms [24].

Finally, we will obtain the results of our analysis having the displacement field both in the X axis and in the Y axis by spatial derivation, as well as the stress field on the specimen calculated based on the strain field on the specimen by means of constitutive models of the material [24].

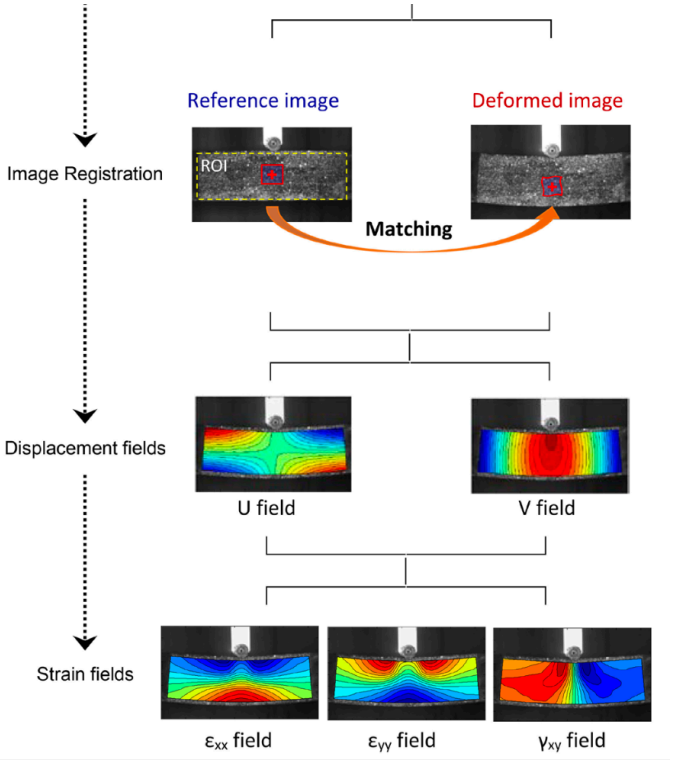

Figure 44 Image Processing using digital image correlation (Source: [36])

It is worth mentioning that the entire process of mechanical tests studied by digital image correlation are well standardized, so there is documentation that will allow us to guide us for a good implementation in hardware, such as the cameras,

the resolution of the image, the angles of the cameras in case of making a 3D DIC, the scale of the image and the speckle pattern, etc., as well as in software and image processing for the creation of the subset and its modification as well as image editing in case better results are required.

For this study we will base ourselves on the manual of *"A Good Practices Guide for Digital Image Correlation Standardization, Good Practices, and Uncertainty Quantification Committee"*, by International Digital Image Correlation Society (iDICs), in its October 2018 version [24].

3.4 Final Comparison Between Techniques for Optical Stress Field Measurement

Once we have finished analyzing all the main options of optical techniques for measuring stress fields, we can make a final review comparing their strengths.

Table 1 Comparison between techniques for optical stress field measurement

	DIC	Photoelasticity	ESPI
Measurement type	Full-field surface strain measurement obtained from image correlation; stresses derived using material models	Direct visualization of principal stress difference through fringe patterns under polarized light	Interferometric measurement of displacement fields with extremely high sensitivity
Material requirements	Applicable to metals, polymers, composites; only requires surface preparation (speckle pattern)	Requires transparent or birefringent materials; not applicable to real structural metals	Requires optically reflective and stable surfaces; no transparency needed but sensitive to surface quality
Complexity	Relatively simple setup and data processing; widely available software tools	Moderate complexity due to optical alignment and fringe interpretation	High complexity; requires precise optical setup, laser source, and phase analysis
Set-up equipment	Digital camera (2D or 3D), stable illumination, image processing software	Light source, polarizers, analyzer, optical setup for fringe observation	Laser, beam splitters, mirrors, vibration isolation system, high-resolution camera
Sensitivity	Good spatial resolution; suitable for small to moderate deformations	Moderate sensitivity; depends on fringe density and interpretation accuracy	Extremely high sensitivity (micro to nanometer scale displacements)
Experimental robustness	Robust under typical laboratory conditions; tolerant to small vibrations and noise	Generally robust; less sensitive to environmental disturbances than interferometry	Highly sensitive to vibrations, temperature changes, and environmental noise
Suitability for bending tests	Ideal for capturing strain distribution, neutral axis evolution, and plastic deformation	Useful mainly for qualitative stress visualization in simplified models	Limited use due to large deformations and instability during loading
Integration into the device under development	Easily integrated using standard camera and lighting system; minimal modification required	Possible with additional optical components, but limited by material constraints	Difficult integration; requires redesign of setup and strict environmental control

Considering that the subject of this study is the development of a 3-point bending test equipment to perform tests mainly on polymers and fragile materials, taking this into consideration we can start by discarding the photoelasticity technique because this technique requires that its specimens be made of translucent materials and its experimental complexity when wanting to mount the system in our bending testing equipment. All this because it has a system dependent on special lenses, polarizing filters and other special equipment which makes it difficult to implement it in our device, in addition to the incompatibility in the materials to be tested.

We can also exclude the technique of electronic speckle pattern interferometry due to its high sensitivity and susceptibility to external disturbances, which necessitates a highly controlled and complex environment, a setup that is incompatible with our device, despite being a technique with very good results.

Finally, we have digital image correlation, which is the most appropriate technique for our case study, this is because the DIC allows us to analyze the distribution of the deformation field along the entire surface of the specimen and due to its high sensitivity, it will allow us to easily identify traction zones. compression and the neutron axis in our bending tests. In the same way, this technique will allow us to analyze the plasticization zones, the concentration of deformation and the nonlinear behavior of certain materials during the tests we carry out [36]. Due to its experimental simplicity we will not require special equipment, but only a white light source and a camera for flat surfaces analysis in 2D DIC, the most important thing to consider will be the fact of creating a good speckle pattern on the surface of the specimen in order to get good results when analyzing the images in a dedicated software for DIC.

4 Build the Equipment for the Measurement

The objective of this Project is to design a piece of equipment capable of performing bending tests and that can validate its results with digital image correlation. For which we must comply with the following tasks:

- Adapt the frame of the old durometer so that it can be adapted to the bending testing machine
- Adapt and fine-tune the mechanical and electronic part of the machine
- Design a controller for the System with which we can control the operation of the machine and obtain results, that is, the resulting graph of Force Vs Deformation.
- Designing the 3-Point Jig for the Bending Test
- Design camera and light mounts to be able to make DIC
- Testing the first prototype

It is known that the specimens with which we are going to work will be mostly made of polymers and fragile materials such as glass. This information is very important since we will be based on their respective standards for the design of the 3-point jig.

4.1 Adapt of the Frame for the Bending Testing Machine

We will start with a frame from a durometer, which will serve us to use its internal components, such as the motor and part of the circuit; and external ones such as the chassis and the tower where the indenter and the table were, so that after adapting it, it can be used as a bending test equipment.

As you can see in the figure below, the chassis of the machine consists of a closed frame of sheet metal, in which all the electronics and controllers of the machine are located inside. Also, inside the box frame we have the motors and the internal vertical actuator. On the actuator and part of the indenter tower we find a solid heavy base which will give stability and resistance to the system to avoid vibrations and unwanted movements during the tests. We continue to see that the tower and actuator section can be opened to access its interior, and in the same way there is a front opening which allows access to the wiring and the relay of the system.

The sheet metal body is intended to support the entire system, which consists of: the motor, the actuator and loading system, the worktable and the supports to perform the bending test and serves to transmit the force to the ground thanks to its wide and heavy base that improves stability and force distribution. It also protects

internal components, preventing interference and unwanted interactions with its components.

Internally the chassis has structural reinforcements in order to avoid deformations of the box during the tests and possible torsion of the frame. In the same way, the chassis and the tower-actuator system is joined by aligners in its heavy base to the chassis and bolts with which we could adjust the system avoiding unwanted movements of the machine and giving greater rigidity to the system.

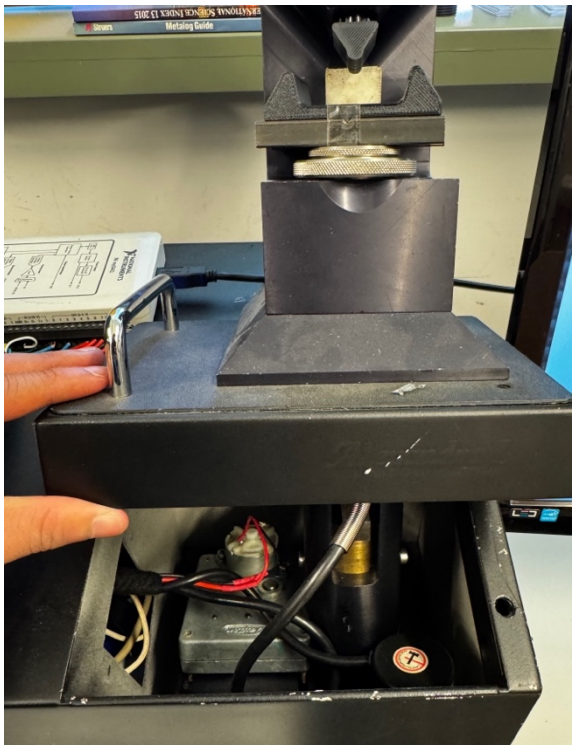

Figure 45 Internal view of the actuator-tower system and heavy base-box frame

The head of the tower where the indenter was located can be disassembled in order to access the internal components of the tower and to be able to add spacers if necessary, modify the thread for the load pin, access internal actuator if required, etc.

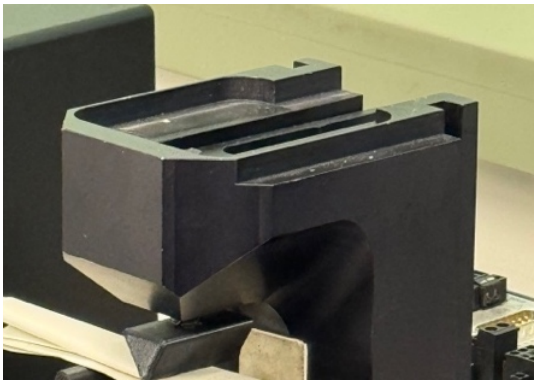

Figure 46 Disassembled tower head

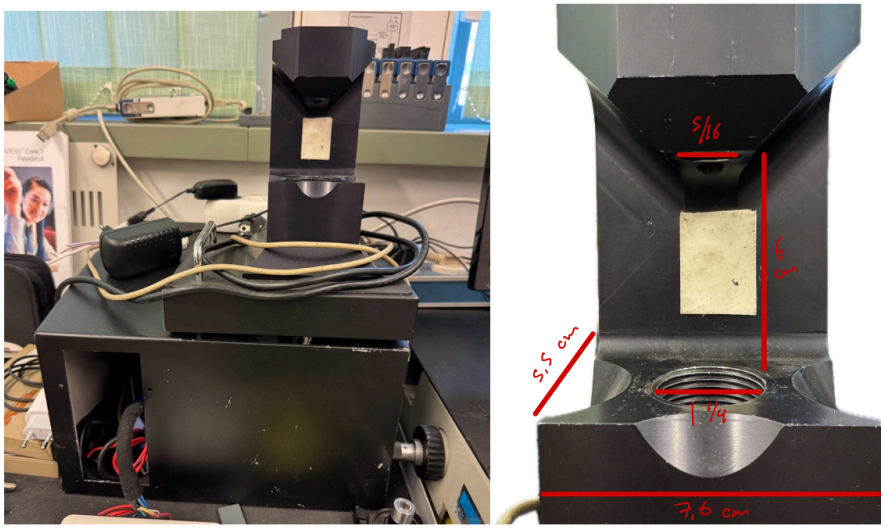

Figure 47 Chassis for the design of the bending testing machine

It should be noted that the working area inside the equipment will be approx. 5.5cm x 7.6cm x 6cm, which is a reasonable space for the size of the specimens with which we will work according to the *ISO 178-2019 Plastics-Determination of flexural properties* standard, and the *ASTM D790-17 Standard Test Methods for Flexural Properties of Unreinforced and Reinforced Plastics and Electrical Insulating Materials* standard.

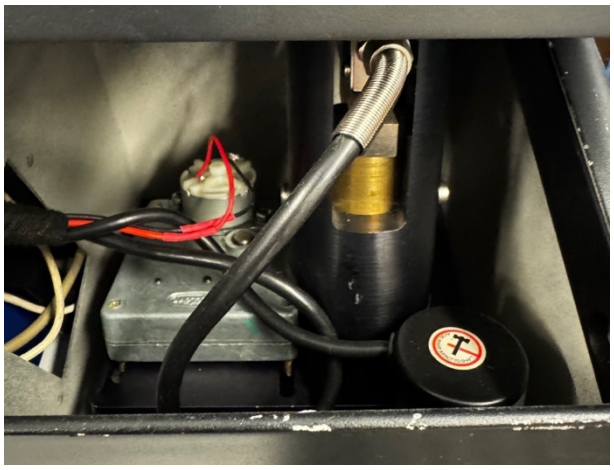

Figure 48 Internal mechanical system of the machine

As can be seen in the figure, under the heavy base and the tower we find the internal actuator which will be responsible for moving the load pin from top to bottom and vice versa, as well as applying the load on the specimen during a bending test on the machine.

The actuator found in this system is an electromechanical actuator based on a screw that will convert the rotational movement of the DC motor present in the system into vertical displacement, which allows the load pin to work during the

bending test, and in turn control it precisely. It should be noted that an advantage of this type of electromechanical actuators is their ability to generate high forces with relatively simple components.

4.2 Adapt of the Electrical Part for the Bending Testing Machine

Knowing that the mechanical system is based on a vertical actuator which is controlled by a DC motor which generates the movement in the load pin, we can make a general diagram of the system already with its electrical connections.

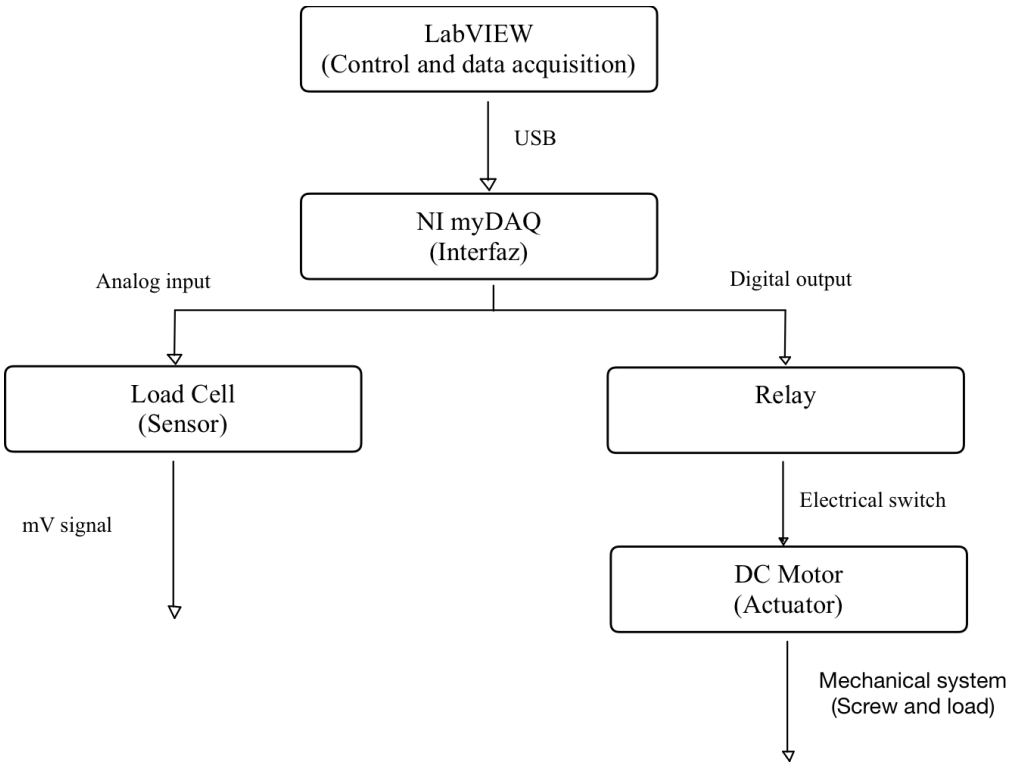

Figure 49 General diagram of the system connections.

As seen in the diagram, the system will be controlled by an application generated in LabVIEW from which we will be able to control the machine both its operation and the collection of data from the bending testing machine. The operation of the machine will be mentioned later.

The LabVIEW program will be operating through an NI myDAQ interface which will be responsible for receiving analog signal reading the signal coming from the load cell in the form of voltage (mV), and will also be responsible for sending digital signal to the relay to turn on/off the machine and control the speed of the load pin through the DC motor control.

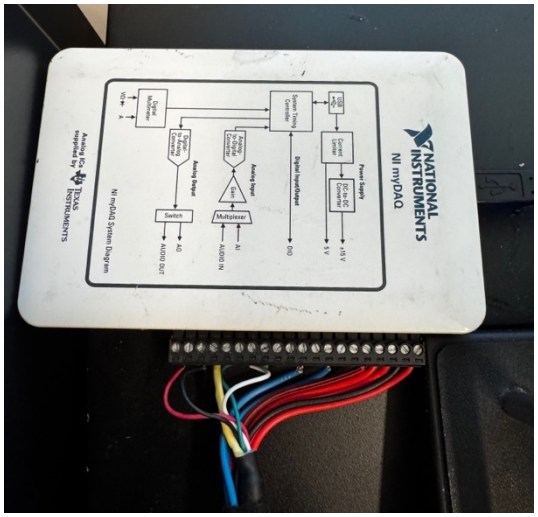

Figure 50 NI myDAQ used to control the machine

The analog signal coming from a load cell which will vary its electrical signal, generally in mV, when a force is applied, this will be in charge of measuring the force during the bending test to later make the Force Vs Deformation diagram. Summarizing the analog signal, the force applied on the specimen during the bending test will be measured by the load cell, which will vary its electrical signal, and this will be read by the NI myDAQ controller and returned to be processed in LabVIEW.

The power source required to operate the sensor and obtain a signal to be able to draw the Force Vs Deformation graph must be above 5V because it was tested and 5V does not deliver a signal but also not above 10V which is the maximum allowed by the NI myDAQ. So, a configuration around 9V is adequate. It should be noted that if necessary, it could also be powered by an external battery.

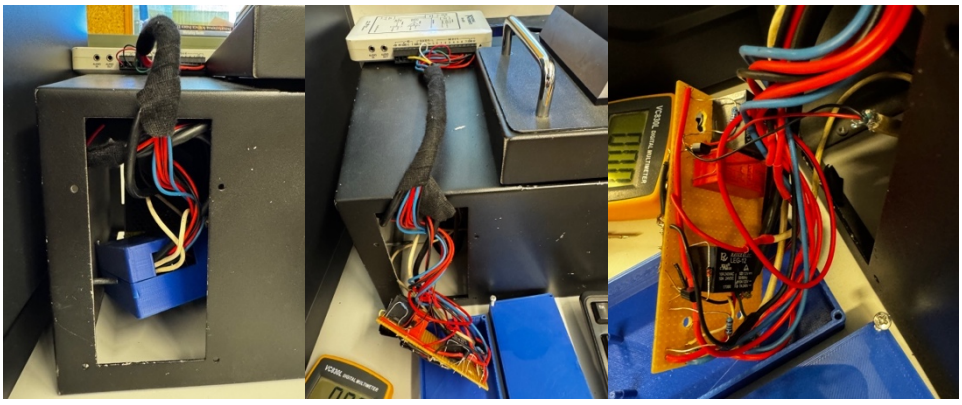

Figure 51 Relay used to control the machine

The digital signal sent from the controller to the relay works as an electrical switch, which will turn the motor on/off, as well as reverse the direction of the screw movement in the actuator causing the load pin to go up or down as needed.

Figure 52 Motor-actuator system that controls the machine

According to the signal sent by the relay, the motor will work in one way or another, turning the screw in such a way that it goes up or down according to what we need. The system rotates the motor, which moves the screw and moves the actuator vertically and finally the load pin goes up or down.

Summarizing the digital signal from LabVIEW we configure the system, which will send a digital signal to the relay causing the motor to rotate in a certain way which moves the screw and makes the actuator go up or down and therefore applying force on the load pin.

4.3 Design of the 3-Point Jig

To design the 3-point Jig it is necessary to first know the samples we are going to work with. We know that we are going to work with polymers, so we know that we are going to use ISO 178 and ASTM D790 standards, Similarly, we are going to take as a reference the commercial model 2810 SERIES MICRO 3-POINT BEND FIXTURE from Instron because it has a load capacity close to that required [20].

According to ASTM D790-17 we know that specimens must be rectangular cross-section so that they remain solid and uniformly rectangular [18].

As said by ASTM D790-17 we know that the dimensions of the specimens will be 12.7 mm (0.5 in.) wide, 3.2 mm (0.125 in.) thick, and 127 mm (5.0 in.) long [18]. And it should be at least 10% longer per side from the span supports.

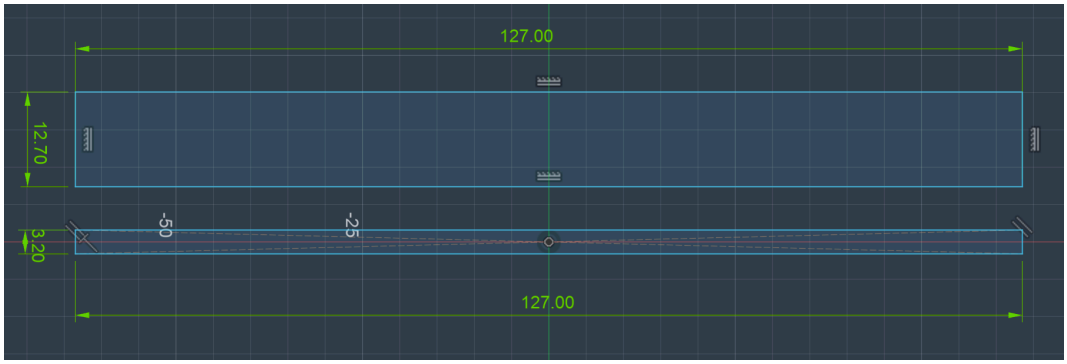

Figure 53 Specimen dimensions

Now knowing the dimensions of the specimens using the standards we will find the diameter that the supports should have, for which knowing that the depth of the specimen is 3.2mm, then we know that the support diameter should be 10mm [18]. While according to ISO 178-2019 the diameter will be equal to 10mm because the depth of the specimen is greater than 3mm [17]

Considering the maximum height of 6cm in the workable area, we can achieve that the 3-point jig for these working conditions will be such that:

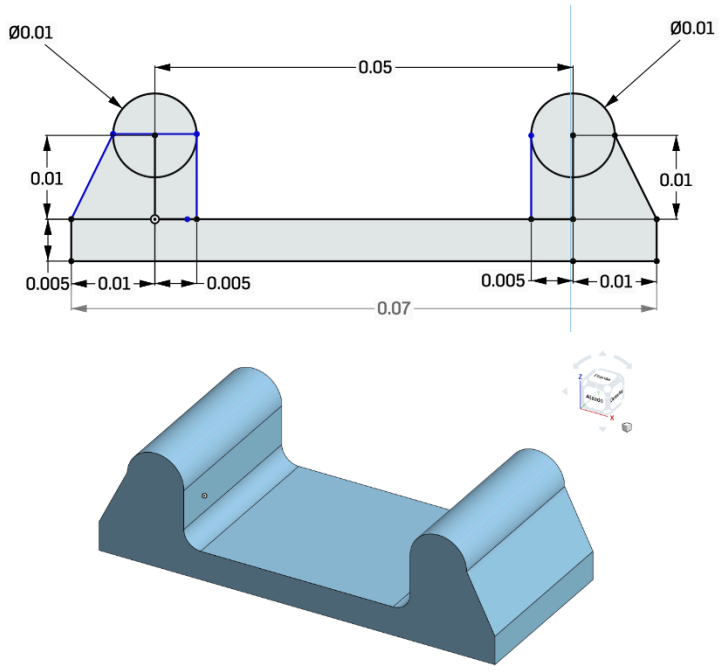

Figure 54 Designed 3-point jig support

The regulations specify a minimum span distance for bending tests, which is based on the thickness of the specimen. As previously mentioned according to the ASTM D790-17 standard, the thickness of the specimen will be 3.2mm, which complies with the relationship established by the standard that the span must comply with:

$$L = (16 \pm 1) * d \quad (18)$$

This results in the normative distance of the span should be 51.2mm. However, considering how impractical it is to handle dimensions with exact decimals at the time of manufacturing, it was decided to select a span distance of 50mm in order to facilitate the manufacture, adjustment and repeatability of the part. In the same way, a distance of 50mm continues to comply with the normative of remaining within a permitted range and complying with the 10% length per side of the specimens, so being a difference of less than 3% does not significantly affect the results and does not compromise the validity of the tests carried out with this piece.

The width of the piece will be about 30mm making a base large enough for specimens of 12.7mm which are the ones we will use according to the normative. The rest of dimensions were selected to fit into the working area.

Continuing with the load pin design, the load applied to the center of the beam must have the same diameter as the support radio [17][18].

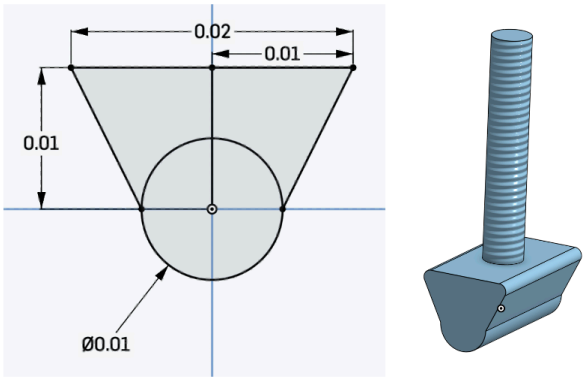

Figure 55 Designed 3-point jig head

Once the parts are ready, they are 3D printed and the pieces are presented together to check the viability of the first prototype.

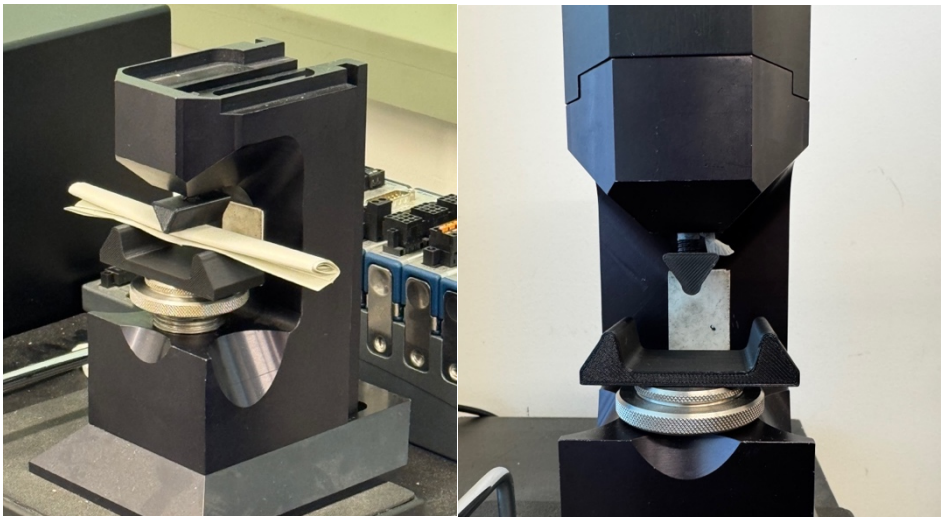

Figure 56 3-Point jig prototype

Once it has been verified that it works, a final version is modeled, adding some improvements to the base model, such as:

- By being able to change the supports, different supports could be designed by varying the span for different types of specimens.
- Modular shape which would allow the supports to be changed to use others of different diameters if required
- A more robust worktable should be made to give greater stability to the bending test supports
- We have to take into consideration the light sources with which we are going to work and the position of the camera to carry out tests
- Modular format to add accessories and change them without major inconvenience

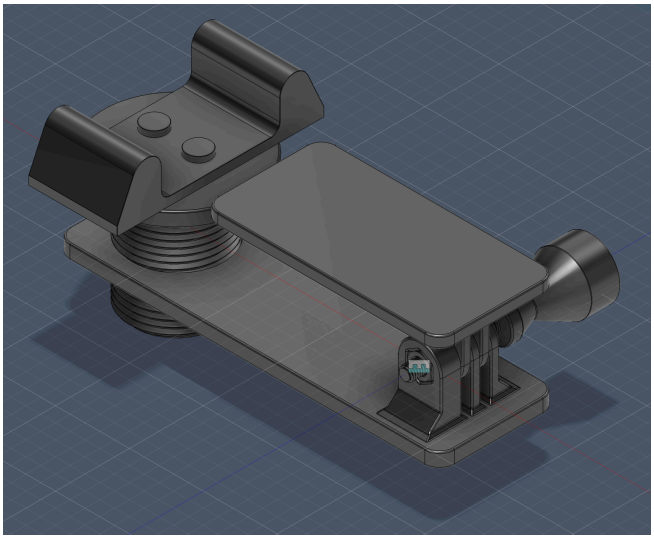

Figure 57 3-Point jig prototype 2 model

The following solution is proposed, which has a modular format and can be modified as needed, starting from the worktable making it more rigid and solid and with bolts which will allow anchoring the various supports for the bending tests with which we could work.

In the same way, an arm was added that can be attached directly to the work base with which it would not alter the bending test area and would allow the addition of various accessories such as lights or a camera directly on the support and thus obtain a stable image during the test.

This arm has a standard attachment of a GoPro camera with which you can get an infinite number of aftermarket accessories to use.

In our specific case in this second model, a second support was attached to the arm where the light that illuminates the specimen in front of the specimen could be directly coupled during the bending test and improving the contrast of the images obtained.

It should be noted that in the existing regulations there is no distance that must be maintained from the light source to the specimen [24], which is considered 15cm sufficient for this model, which also leaves enough distance so that, depending on the type of light source we use, it emits heat and does not alter the bending tests or the taking of images.

Figure 58 LED light used for our DIC equipment

As can be seen in the figure, a standard white LED light was chosen for our DIC equipment, which will be fitted to the arm and pointed directly at the specimen, thus illuminating in a better way and allowing a greater contrast between the speckle pattern and the background.

Because the dimensions of the support rollers were not changed, the charging pin maintains its original dimensions and shape. This is only necessary to change in case we change the rollers and the dimensions of the support in the same way to perform other bending tests on different types of specimens.

5 Develop a LabVIEW Based Software for Measurement and Evaluation

LabView is a development environment created by National Instruments, which allows you to develop applications for automation, control and measurement systems based on their own equipment, as in this case we are using an NI myDAQ controller. LabVIEW uses a graphical interface allowing applications to be created in a more intuitive and visual way.

Remembering that our system is contained in the controller that sends a digital signal and reads an analog signal, a relay with which we will control the direction and speed of the screw rotation, a DC motor, the screw which will produce vertical movement in the actuator and therefore will be in charge of applying the force for the bending test.

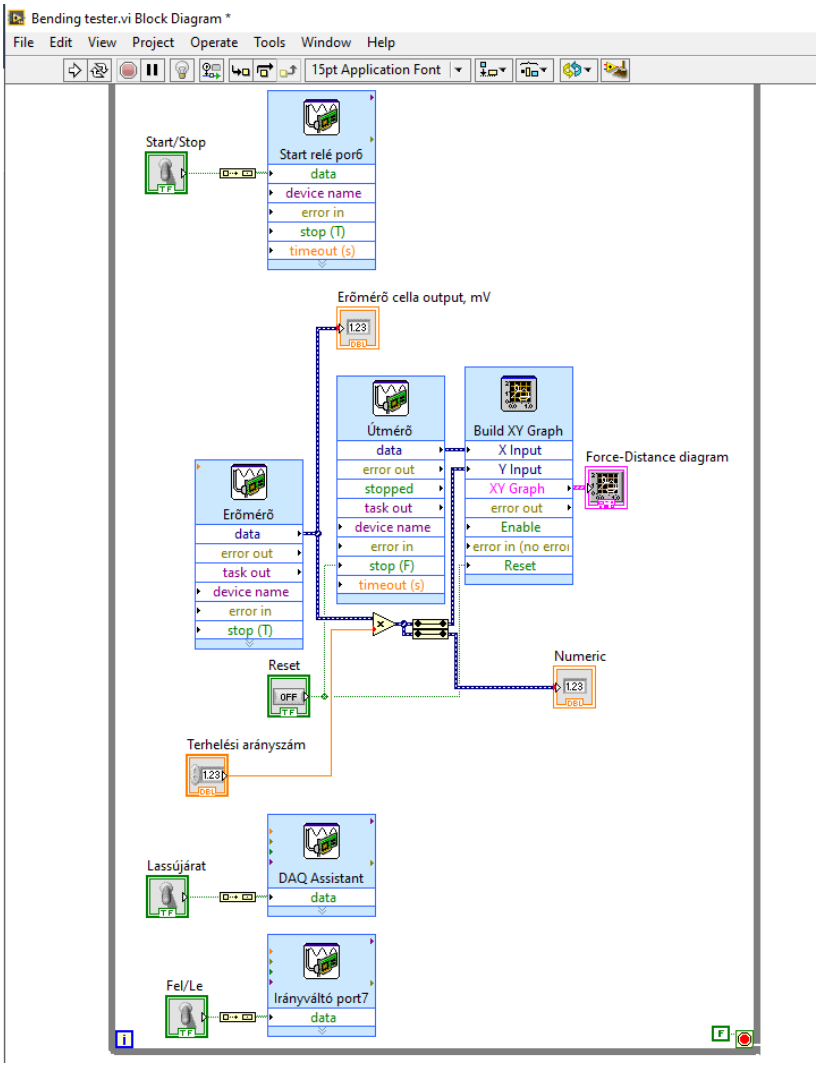

Figure 59 Program block diagram in LabVIEW

Taking into consideration the elements of our system, a block diagram was designed in LabVIEW which allows us to control this equipment and obtain results from it.

The main function of the program is to control the system by being able to raise, lower and control the speed of the load pin, as well as obtaining data from the bending test and giving us a resulting graph, in this case the Force Vs Deformation graph.

The operation of the block diagram is mostly based on the *DAQ Assistant* block which receives the analog signals from the *NI myDAQ* controller thus making a simplified data acquisition and control limiting a little the control options that we could acquire with other tools within LabVIEW but being effective enough for the function we want. The program runs in a continuous cycle where data is read, and indicators are updated in real time.

The data received obeys with a linear scheme, that is, as they enter, they are processed in their respective blocks and then returned for visualization by means of the indicators presented in the system or the resulting graph. As can be seen in the block diagram we have four indicators, three of them being a numerical indicator, an indicator of output of the load cell in mV and another number of load ratio, this being editable by the user and useful to control the values shown in the graph. In order, the fourth indicator will be the Force Vs Deformation graph.

About the actuator, the diagram shows switch type actuators; that is, each control button sends a direct signal to the relay and, consequently, to the actuator. There are three switches in the system: one to turn the machine on and off, one to change the direction of the load pin's movement, that is, to go up and down in relation to the test specimen; and a third switch that controls the advancement speed, providing a fast mode and a slower, safer mode for certain applications.

Regarding safety during the bending test, the equipment has direct controllers, so the on and off button also serves as an emergency stop. A reset button is also presented for graphing and data acquisition with which any erroneous reading or malfunction could be eliminated and start with a new data collection without the need to stop the program.

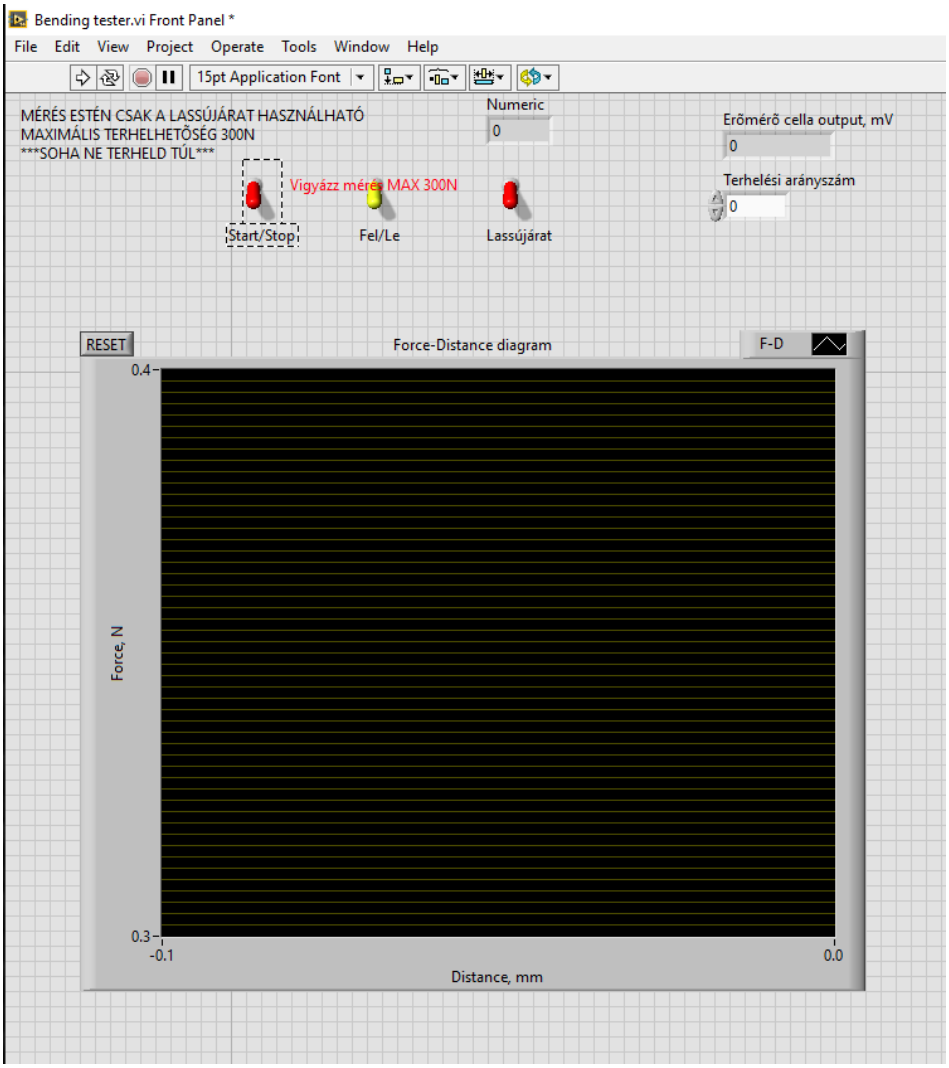

Figure 60 Front panel of the program in LabVIEW

On the front panel we can see the interface created that consists of the three switches, one that turns the machine on and off, another that depending on the position raises or lowers the load pin, and the third which consists of the normal or slow speed mode for greater safety during the test.

There is also the reset button that will serve to clean the data on the screen and avoid saving noise data or data taken incorrectly during the test.

In the same way we can see the 3 indicators, the numeric, the load index which is editable by the user and helps us to calibrate the machine and maintain a stable reading without major noise; and the indicator of the power cell output which is in mV.

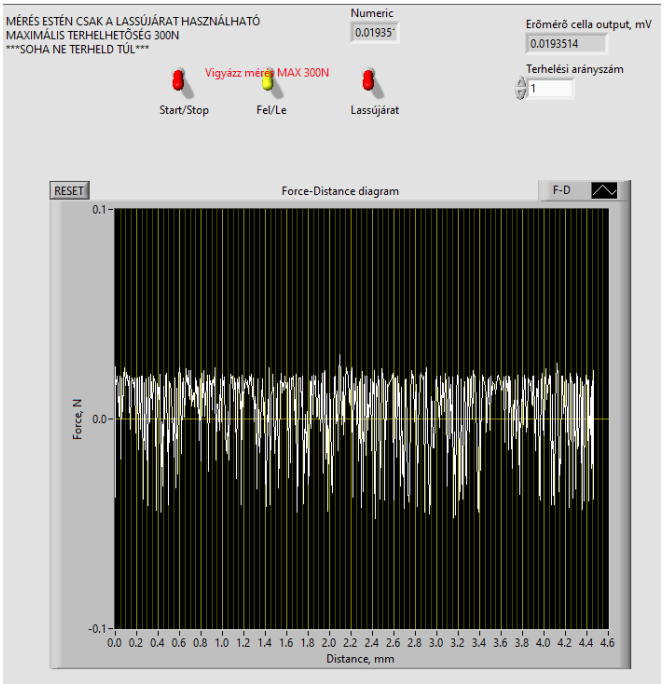

Figure 61 Noise present in the received graphic.

In the figure we can see the graph resulting from a function test without a specimen placed, that is, only to see the movement of the load pin, We can notice how the force on the graph remains close to zero however the important thing to note here is how this graph presents a lot of noise. We have to reduce the noise we get from the system probably coming from cables, connections or the system that is not properly calibrated.

It is planned in the future to use a strain gauge to be able to correctly calibrate the load pin using the load index factor editable by the user to obtain a stable and noise-free signal, also ensuring that we obtain a value closer to reality in the results obtained in the graph.

Finally, we have a large screen that will be in charge of showing the Force Vs Deformation graph in real time during the bending test.

As you can see, the front panel is fully labeled in each of its functions and indicators and is highly intuitive for use by a person outside the project present here.

6 Summary of the Results

6.1 Set Up Designed for the Bending Testing Machine and Analysis Using Digital Image Correlation

In the image below we can observe the final assembly of the functional bending testing machine connected to the controller in LabVIEW to collect data through the sensors connected to it from where we will obtain the Force Vs Displacement graph.

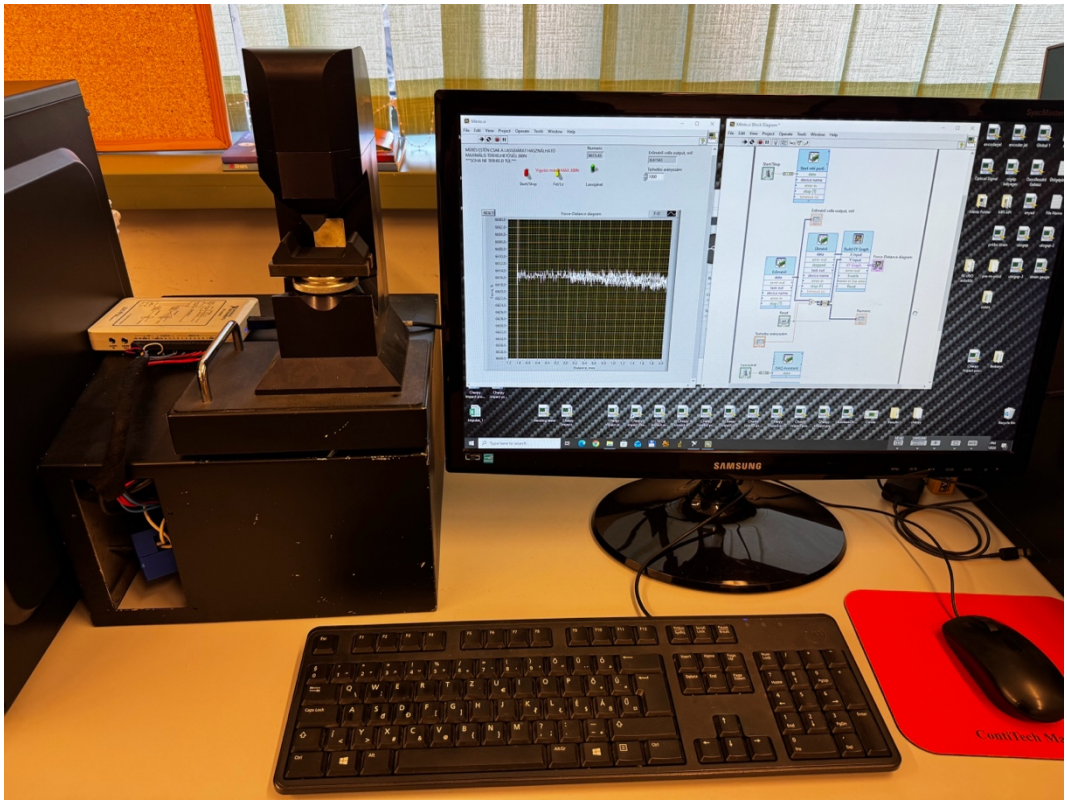

Figure 62 Final set up of the bending testing machine and the software

Then we will show the set up used to obtain images and the study by digital image correlation, which will serve to complement the results obtained through the testing machine and the program in LabVIEW.

As mentioned previously, in order to perform an analysis of stress fields using digital image correlation, we will basically need a camera with which we will obtain a video or a sequence of images of the bending test carried out and an illumination equipment which will give us a good contrast in the speckle pattern and the background.

The assembly consisted of a traditional white LED light located about 20 cm away and which was pointed directly at the specimen during the bending test.

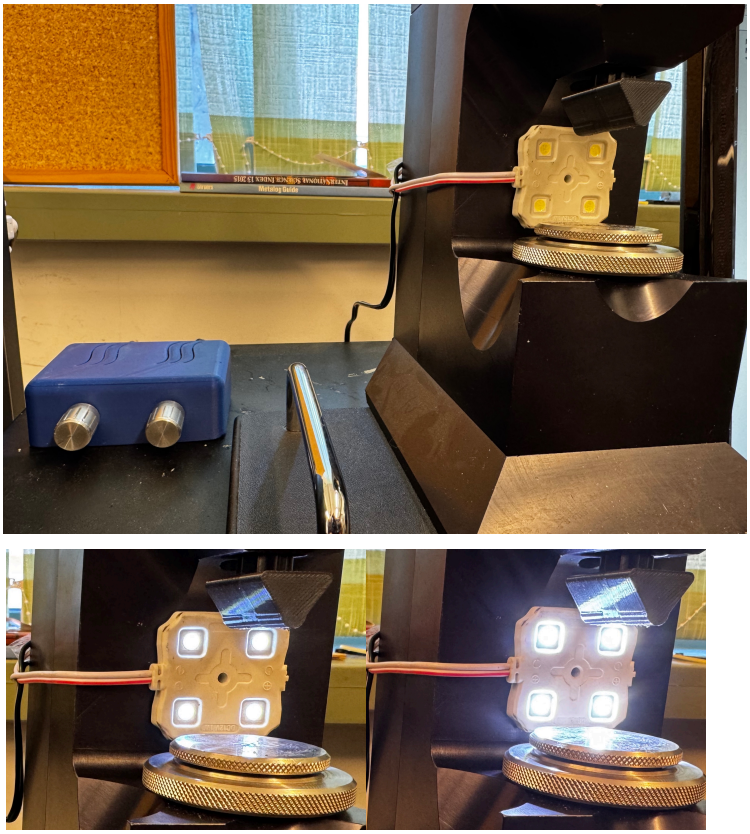

Figure 63 LED light used for the DIC

As can be seen in the figure, the white light source was connected to a potentiometer from which we can control the intensity of the light we want for our experiment. This will be very useful to find the perfect contrast and the best image quality that we can get from the speckle pattern with the camera we use. The position of the light source shown in the figure is not the position in which the tests were performed, it is only an illustrative image.

To obtain images of the test, a Sony Cybershot DSC-QX10 camera was used, which can be wirelessly connected to the computer from which we controlled the camera while the flexion test was being performed.

Figure 64 Camera used for the DIC

The selected camera configuration was to take a video at 4K and 60 fps of the bending test, this represents that the images obtained are too heavy, however, the images were later processed to reduce their weight and improve the image quality, this will be discussed later.

6.2 Preparation of Specimens for Bending Test

In the same way, we will begin to prepare the samples with which we will test a three-point bending test and in turn we will test the set up to perform DIC with these.

For the tests carried out, transparent polystyrene sheets were used as test material. Due to the fact that the plate of the material used was of a thickness less than that indicated by the regulations we used to design the system, the dimensions of the specimen had to be changed, with which we obtained new specimen dimensions according to the ASTM 790-17 standard with specimens of dimensions of 1.5mm thickness, 12.7mm wide and 60mm long.

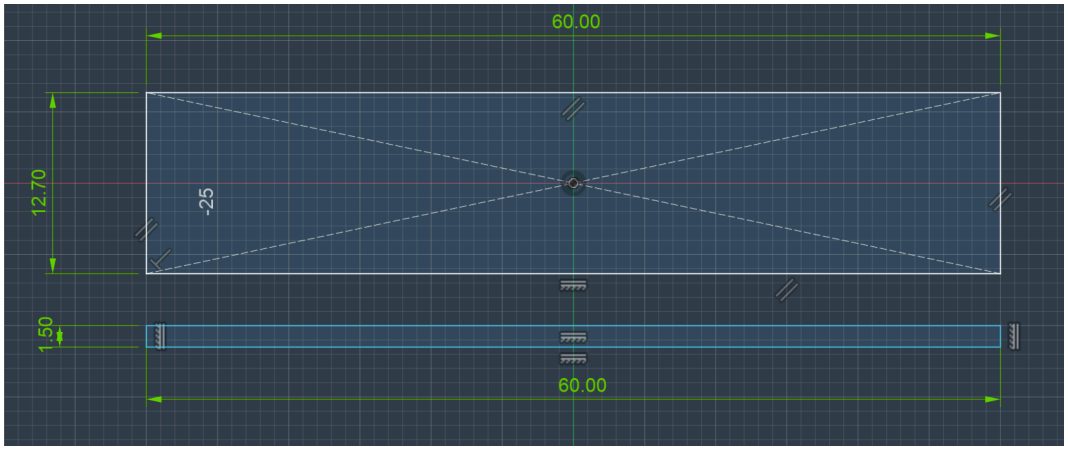

Figure 65 Dimensions of specimens used in bending tests

With the available material, 18 specimens were prepared cut according to the new dimensions.

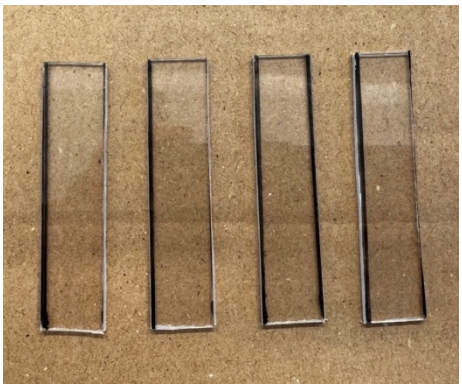

Figure 66 Polystyrene specimens used during the test

The specimens were prepared according to the regulations provided by the *International Digital Image Correlation Society* in its manual A *Good Practices Guide for Digital Image Correlation,* whereupon the specimens were sanded and polished to clean any surface defects present by the cutting of the material, and then thoroughly cleaned to remove any stains or elements that may alter the follow-up of the speckle pattern during the analysis of digital image correlation [24].

Once the specimens are clean and prepared, the speckle pattern was applied on their flat surface, which is of interest for the bending test and which will be analyzed by 2D DIC. The speckle pattern was applied according to the procedure established by *Correlated Solutions* where the appropriate way to apply a speckle pattern is established, maintaining an adequate distance between points, randomly placed points and respecting a correct distribution of 50-50 on the surface. In the same way, it was checked that the pattern placed does not present lines or that they do not present uniformity in the size of the points on the surface that can alter the point tracking procedure through the specialized software for digital image correlation [37], in this case we will use an open-source code that runs on MATLAB called Ncorr.

Figure 67 Speckle pattern applied to the surface of the specimens

6.3 Image Acquisition During the Bending Test

Once we have all the equipment prepared and the specimens ready, we will proceed to perform the bending test while we take data and images by DIC.

The camera recorded a video of the bending test at 4K and 60 fps with which we made sure to obtain a great image quality and a good image of the speckle pattern in each of the frames that the test lasts. From this video we can rescue two special frames which are the first frame that shows the specimen in its initial condition called reference image, and the last image showing the maximum deformation of the material before fracturing or reaching the maximum capacity of the machine, which is called deformed image.

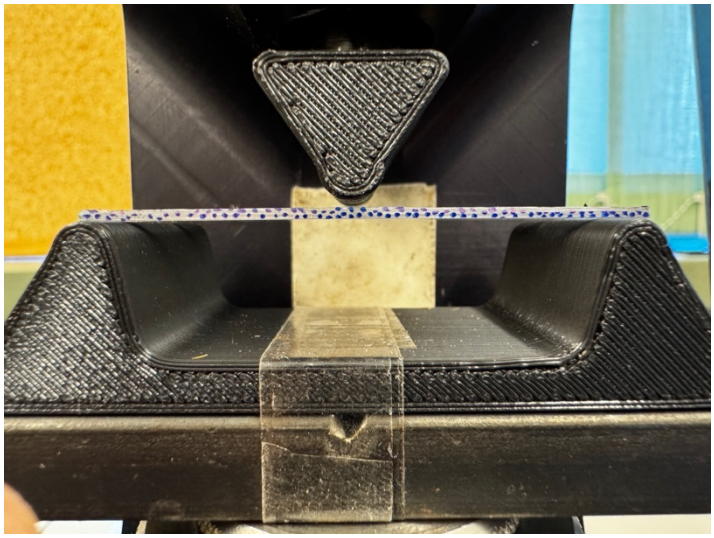

Figure 68 Reference image of the bending test

The reference image will be used to compare each of the frames of the video with it and thus obtain the offset of each of the points in the speckle pattern.

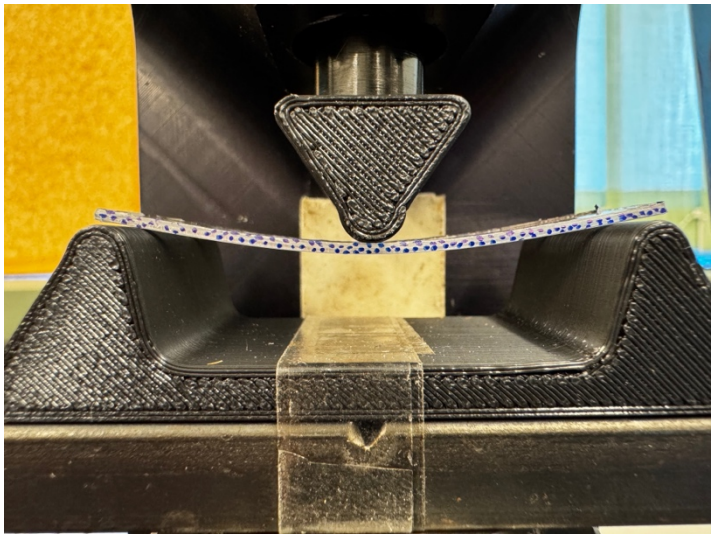

Figure 69 Deformed image of the bending test

The deformed image shows the maximum point reached during the test and serves to indicate the maximum values reached and analyze displacements and strains.

6.4 Image Pre Processing

Observing the images obtained we can notice that the study area is very "far away" from the focus of the camera so we will need to perform a preprocessing of the images before performing the digital image correlation analysis.

In this studio, ImageJ is used for the pre-processing of the images. First we have to consider that since it is a video or a single sequence of images of the same event, all the images are supposed to be in the same camara´s frame, that is, that the camera did not move and therefore the positions of the objects within the camara´s frame should coincide in each frame of the video or images sequence. With this in mind, we start as a first step to make a crop in the image reducing unnecessary information from it. In this case, we will isolate only the area where the bending test is carried out on the specimen.

Figure 70 Cropped image from reference image

By reducing the information present in the image in this way, the specialized digital image correlation program does not waste time analyzing unnecessary information. In the same way, we can better isolate the speckle pattern from the surface of the specimen, making it easier to track the points by reducing the cost of computational power, improving stability and preventing the program from trying to correlate regions that are not relevant and could only lead to analysis errors.

The next step will be to apply a threshold filter on the image which will turn the image into a black and white image. This step will convert the image into a continuous grayscale which forces a greater separation between light and dark areas and therefore creating greater contrast in the image, which will allow us to identify the speckle pattern in a better way and be easier to track for the digital image correlation analysis program.

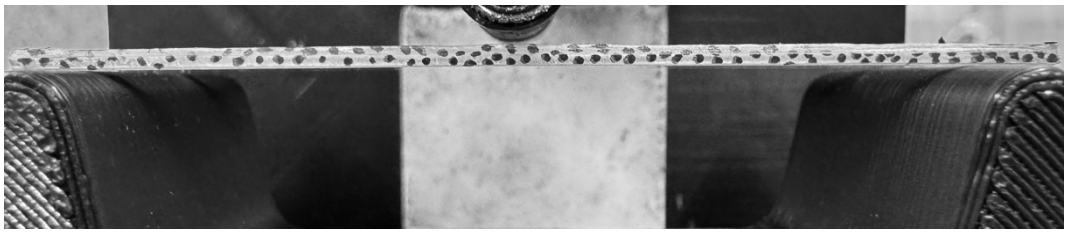

Figure 71 Reference image passed with the threshold filter

The disadvantage of performing this step is that in certain cases when using the filter information is lost in the image, and in cases where the speckle pattern is poorly done or the image quality is not sufficient, several points will be lost and therefore difficult to track the speckle pattern.

The next step will be to convert the images into 8-bit images reducing the size of the data with which we make the analysis of the images through the digital image correlation software more effective and faster. Similarly, this step ensures that the images are compatible with most image analysis programs for digital image

correlation and many codes in MATLAB which generally work with 3-channel images (MxNx3), without losing too much resolution in the images while maintaining an intensity, generally, of 256 levels making them good enough for analysis.

The final step will be to convert the images back into RGB format images which are images with a 3-channel format (MxNx3), which will also serve to ensure the compatibility of the images with most codes in MATLAB and most image analysis programs for digital image correlation. This step will not change the quality of the image, but it ensures that there are no formatting errors with the software.

As mentioned in a beginning, for this pre-processing of the images we used ImageJ, which we could save a macro of the processing of the reference image that we did and automatically run with the rest of the sequence of images that we will deal with, thus simplifying the processing process and the images and automating it in a certain way so that at the end of the process we get all the images cropped in the same region, selecting the same filters and converting them in the same way in order to be able to export the preprocessed images at the same time.

6.5 Image Analysis Using Digital Image Correlation Using Ncorr

For the analysis of images using digital image correlation for a flat surface in 2D, the DIC analysis software called Ncorr will be used. This is an opensource program based on MATLAB to perform image analysis using 2D digital image correlation [39]. The theory behind the code and how it performs the speckle pattern tracking and gets results are beyond the scope of this study so it will not be mentioned. The functioning and operation of the program will be based on its official operations manual available on its website *ncorr.com* [39]

Ncorr presents a very intuitive interface which will guide us step by step to be able to perform a DIC analysis with the images we upload.

Figure 72 Ncorr Interface

As can be seen in the upper left part of the Ncorr interface, we can see the steps that we must follow to perform a DIC image analysis, which is easy to follow the process and there it will mark the pending steps and those that were successfully performed.

The process begins by uploading the reference image and setting it as the initial image of the image sequence. In the same way we must upload the current image which will be the deformed image that we had previously mentioned. When loading the deformed image, we can upload the complete sequence of images or a single final image of the result of the bending test. During the analysis the program will compare each of the uploaded images with the reference image.

Figure 73 Reference image and deformed image uploaded to Ncorr

The next step will be to select the region of interest on the surface of the specimen to carry out the study on that area. In this way we select the area in which we want the program to follow the speckle pattern and ignore the parts outside of it, thus avoiding areas without deformation or background images.

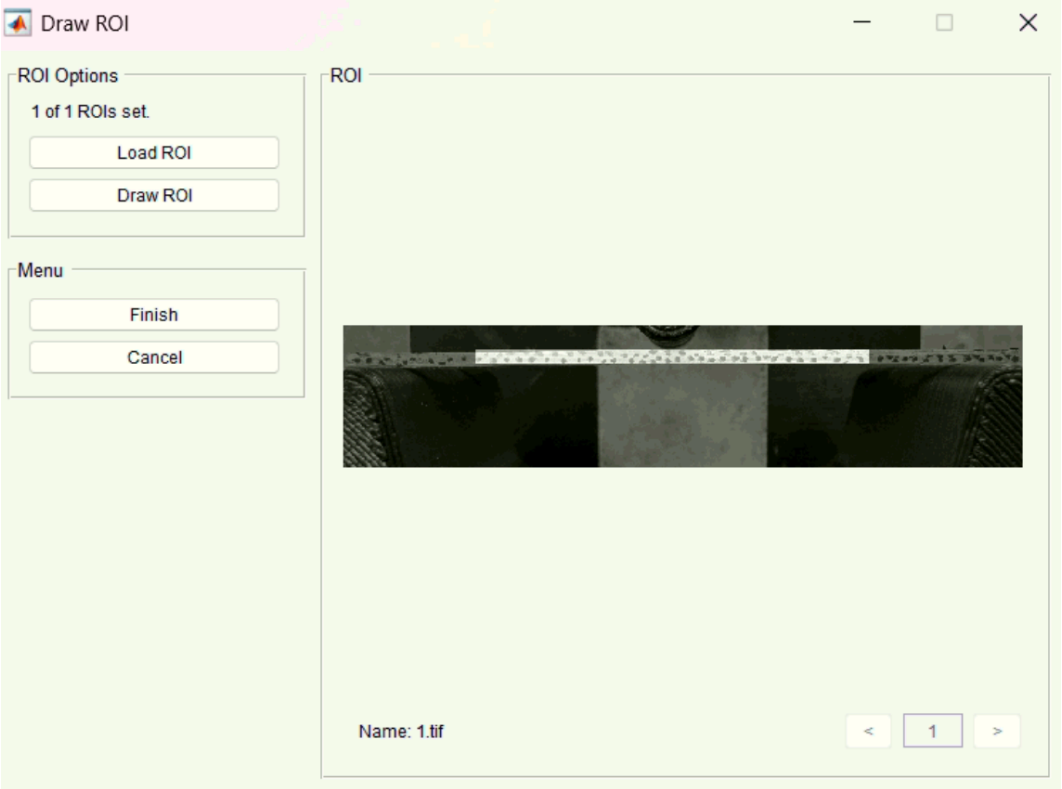

Figure 74 Selection of the region of interest for the study of DIC

Ncorr has several tools and ways to select the region of interest for the analysis of DIC on the selected images, however, for our study of a three-point bending test we only want to study what happens in the specimen, so we will select a rectangular region along the specimen which contains the speckle pattern inside. It should be noted that the selected region will be maintained for all uploaded images and for the rest of the analysis process.

Figure 75 Region of interest selected for this study

The next step will be to set the parameters for the DIC where the subset is going to be selected and configure it in case we want to change it to certain specific measurements. The subset are small cells within the region of interest which each one has a unique pattern of pixels or points within its cell, which the program will divide and when comparing the deformed images with the reference image the

program will look for these cells and their unique pixel pattern within the deformed image and thus be able to compare their initial and final position thus obtaining their displacements.

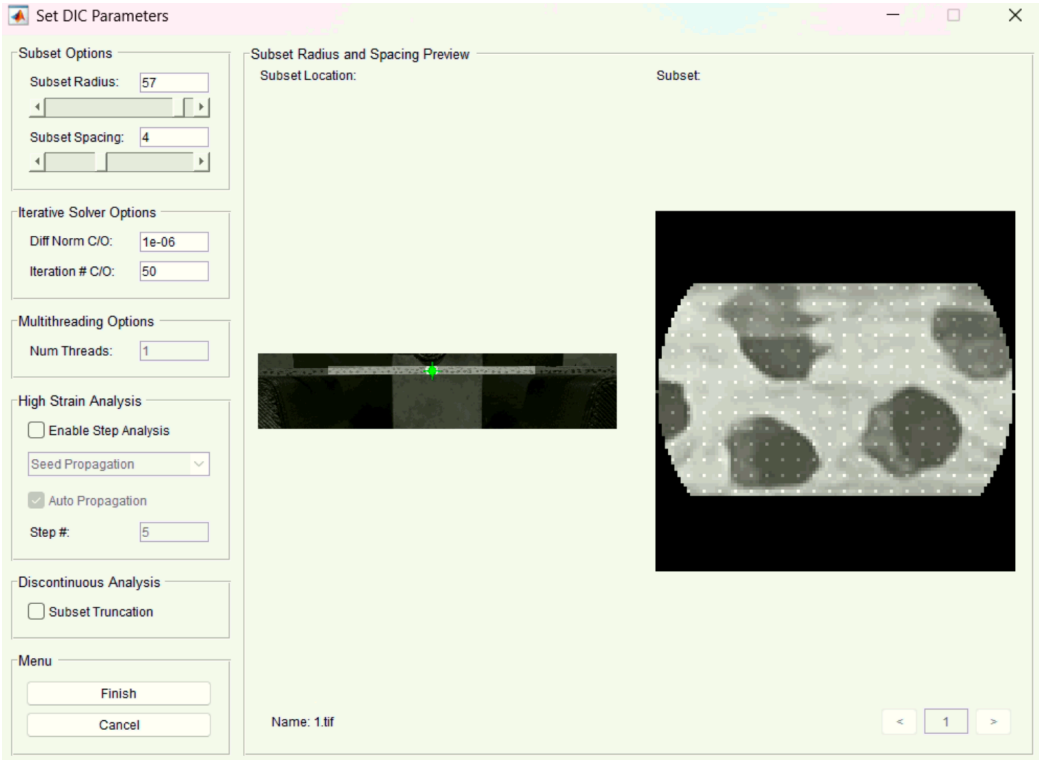

Figure 76 Set DIC parameters on Ncorr

It must be considered that the smaller the selected subset the more information we could obtain in the results, however, this means that the images must have enough quality to be able to identify each of the pixel patterns in each cell and also of a high computational power that can handle all the offset values for each cell.

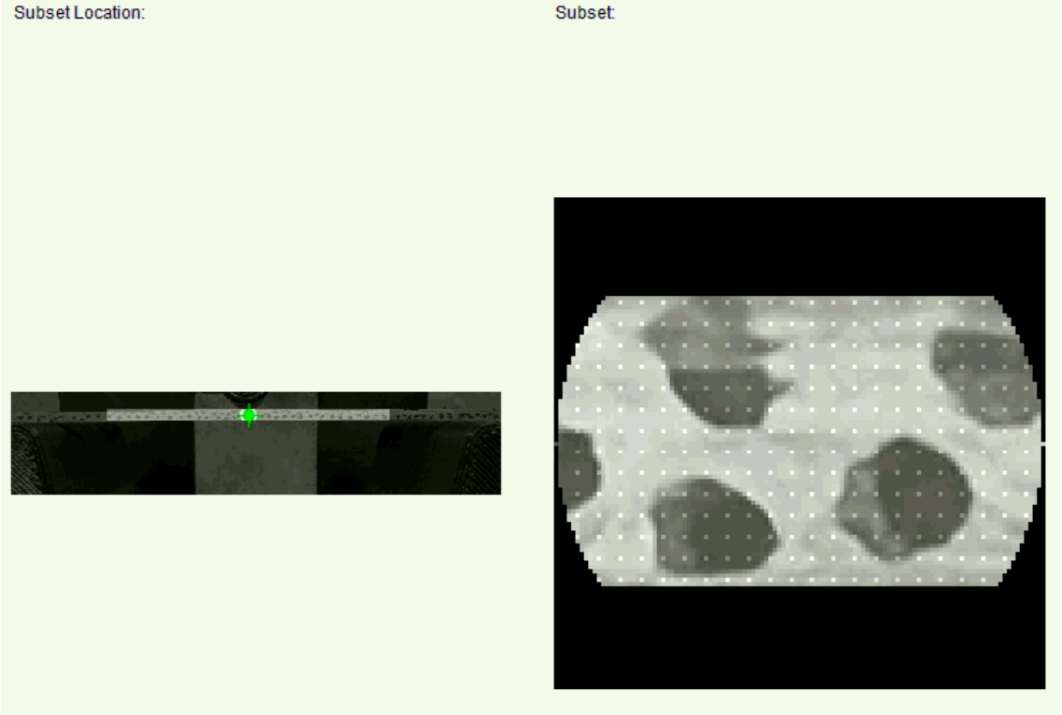

Figure 77 Subset selected for our DIC test

To exemplify the operation of the subset, the image on the right in the figure represents one of the subsets that Ncorr has chosen from the region of interest, the image on the left shows the position of this specific subset within the region of interest. During the analysis of digital image correlation, what Ncorr will do is look for this same pattern of dots and pixels of the speckle pattern throughout the sequence of images, once it finds a match in the deformed image what it will do is take that point and compare it with the reference image and compare the two images to see how much the subset moved between images.

Once we have defined the region of interest and the optimal configuration of the subset, the next step will be to perform the DIC analysis. Here we will select which correlation algorithm we want the software to use to identify the patterns and how the subsets will compare between images.

Once the DIC analysis is finished with the images and configuration selected, the program will return a preview of the results of displacements on both the X and Y axis, and here we can configure a scale on the image. For example, for our specific case we can select the thickness of the specimen as a known distance and the program is responsible for sizing the images at that scale in relation to pixels.

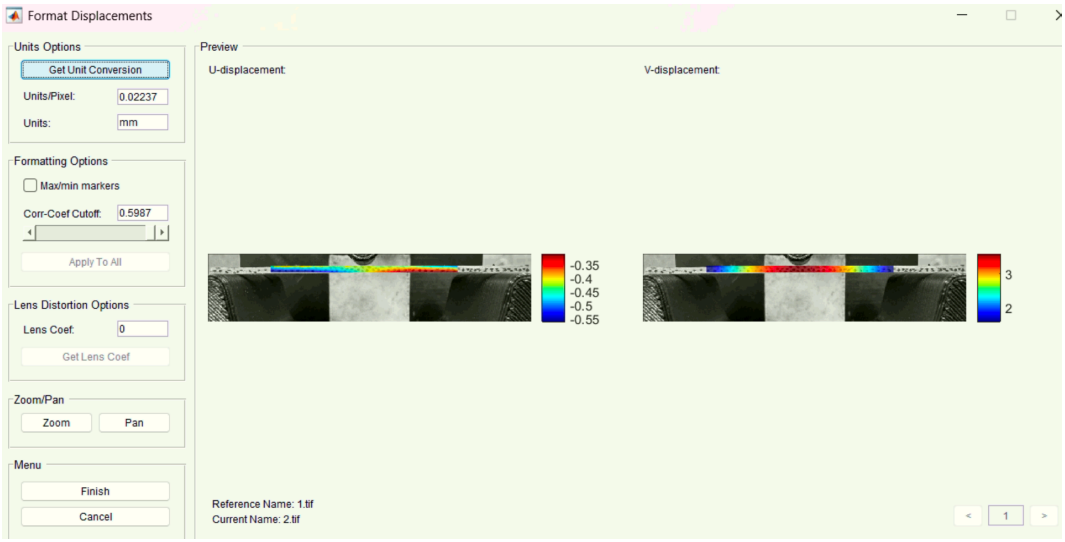

Figure 78 Preview displacement results and set a scale in the image

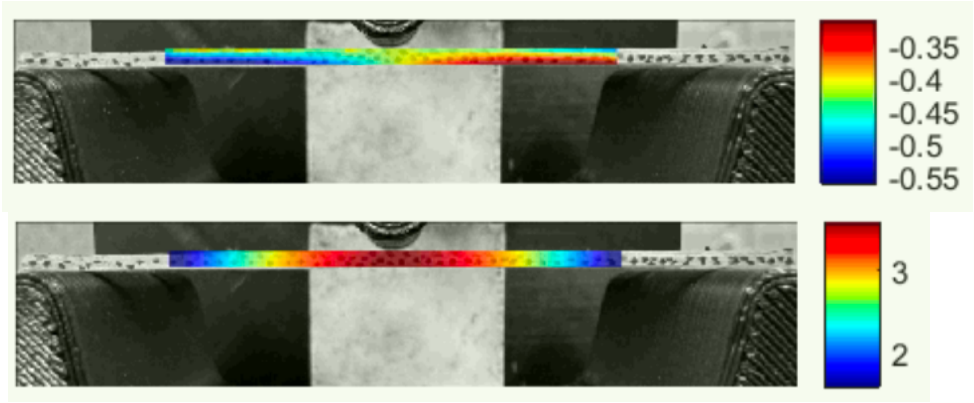

Figure 79 X-axis and Y-axis displacement results on the reference image

Here we can make a parenthesis to comment on how all the configuration of the digital image correlation analysis is being carried out on the reference image, such as the selection of the region of interest as well as the setting of the scale and configurations of displacements and strain. This is because all the following images of the sequence that we have uploaded will be compared with the reference image, making this a kind of constant on the entire analysis and starting point and comparison with the rest of the images [39].

Once the results of displacements have been defined and a scale set on the images, the next step will be the configuration of the strain, where we will be able to observe a three-dimensional graph of the displacement over the entire surface selected as the region of interest. These results could vary by making them more detailed by reducing the radius of the strain, making it so that for example, in the image settings below a very high radius is shown in order to show all the displacement within the entire region of interest; however, in case we want only the displacement on the tip or at a specific point in the area of interest, we could reduce the radius and select that region that we want to observe in the graph. The strain

calculated by analysis is obtained based on the calculated displacements which will be used to calculate the spatial derivatives and thus obtain the strain.

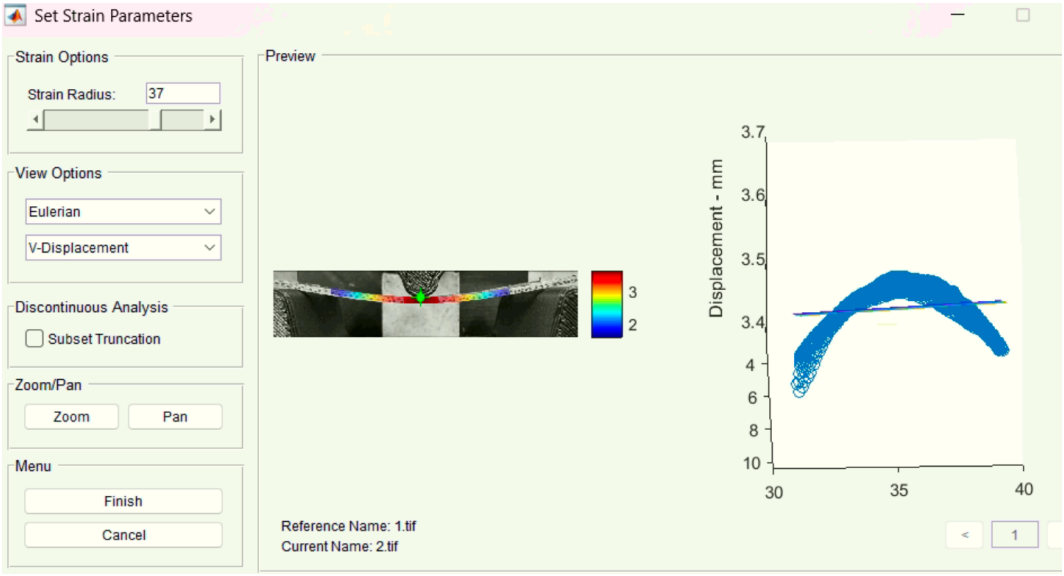

Figure 80 Set strain parameters

In the same way, there we could preview the displacements both in the reference image and in the deformed images of the sequence of images that we have loaded for analysis.

Finally, with everything configured and with the analysis carried out, we will be able to observe the results of the analysis for both displacements and strain in all axes and in all frames of the image sequence loaded for the study.

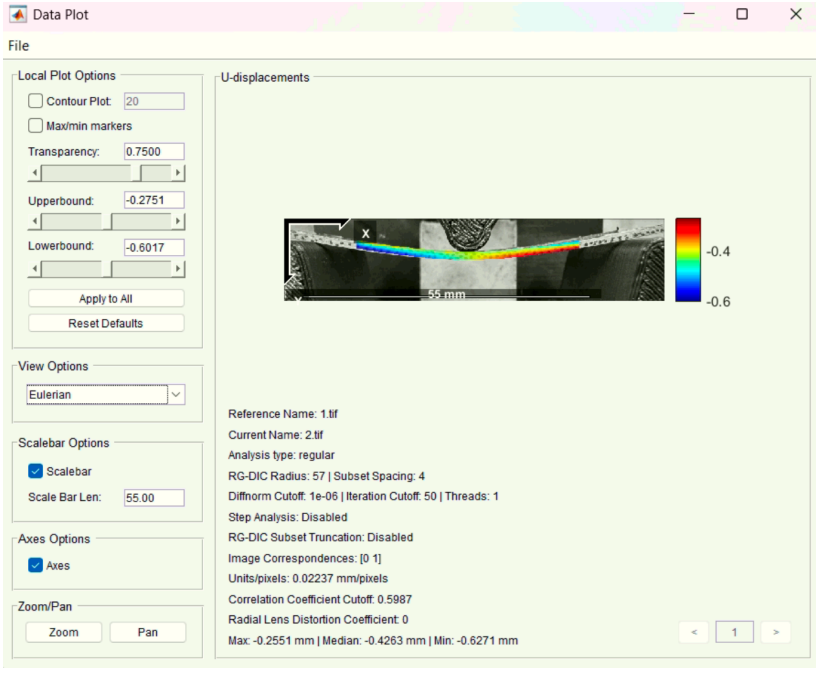

Figure 81 Ncorr displacement results display window

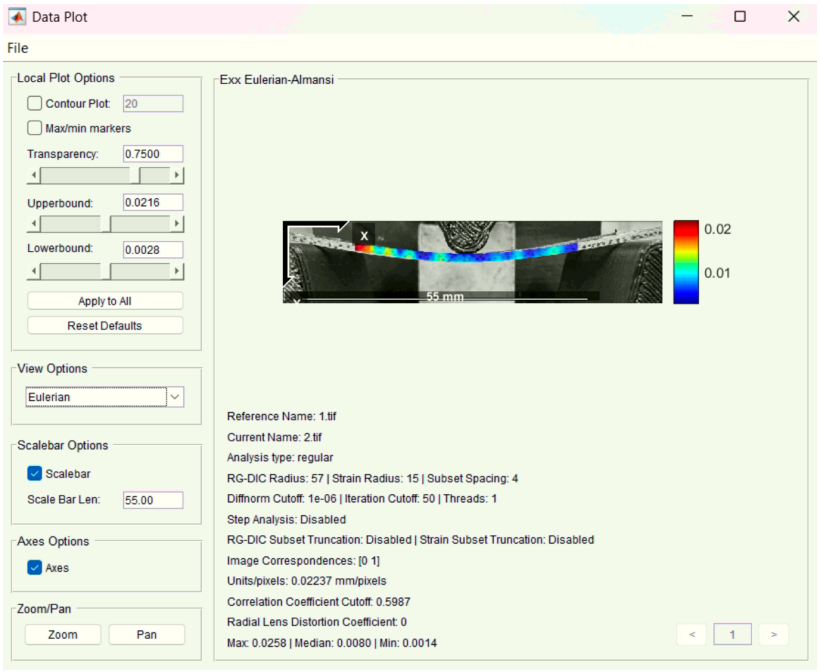

Figure 82 Ncorr strain results display window

6.5.1 Displacement Results

Once the digital image correlation analysis is completed with the set of images loaded from our bending test performed on our bending testing machine to transparent polystyrene specimens according to the ASTM 790-17 standard for the preparation of the samples and the supports used during the test, and following the regulations provided by the *International Digital Image Correlation Society* in its manual A *Good Practices Guide for Digital Image Correlation*, we can analyze the results obtained using the digital image correlation analysis software called Ncorr.

In the image below we can see the analysis result that shows us the displacement in the X axis that the specimen suffered at the end of the bending test performed. At the top we can see the result on the region of interest in the reference image and at the bottom the result of the DIC analysis on the distorted image. During this test, it is expected that the displacement in the X-axis will be extremely less than that present in the Y-axis.

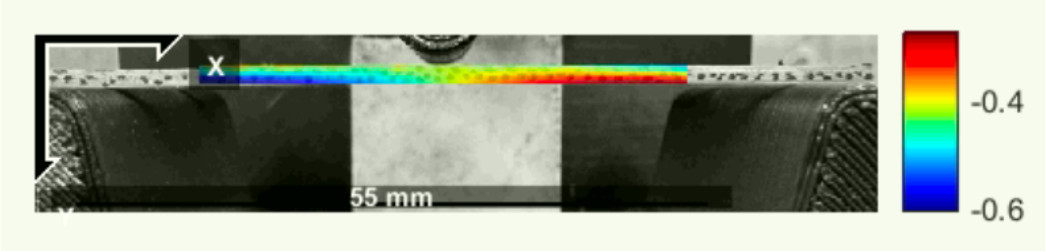

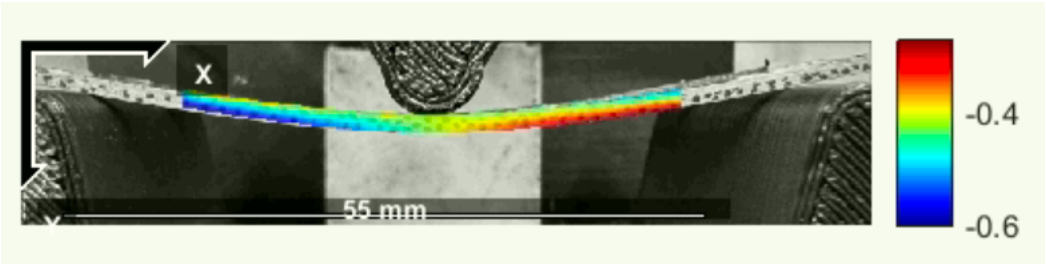

Figure 83 X-axis displacement results in the reference image and in the deformed image

We can see how the result indicates that there was a maximum displacement in the X-axis of 0.6mm, which is an acceptable value considering that the displacement in the X-axis is generally due to the curvature presented by the specimen and the geometric effect of bending during the bending test. The value of the displacement is negligible, which can confirm that there were no errors in the assembly of the specimen that represent that the specimen slipped on the supports during the test.

In the image below we can see the analysis result that shows us the displacement in the Y axis that the specimen suffered at the end of the bending test performed. The Y-axis displacement results are the strong point of this analysis, as this is where we can see the deformation suffered by the material during the test in its main deformation. The expected results for this analysis are a greater presence of deformation in the center where the pin load was applied, until it approaches a minimum deformation towards the supports.

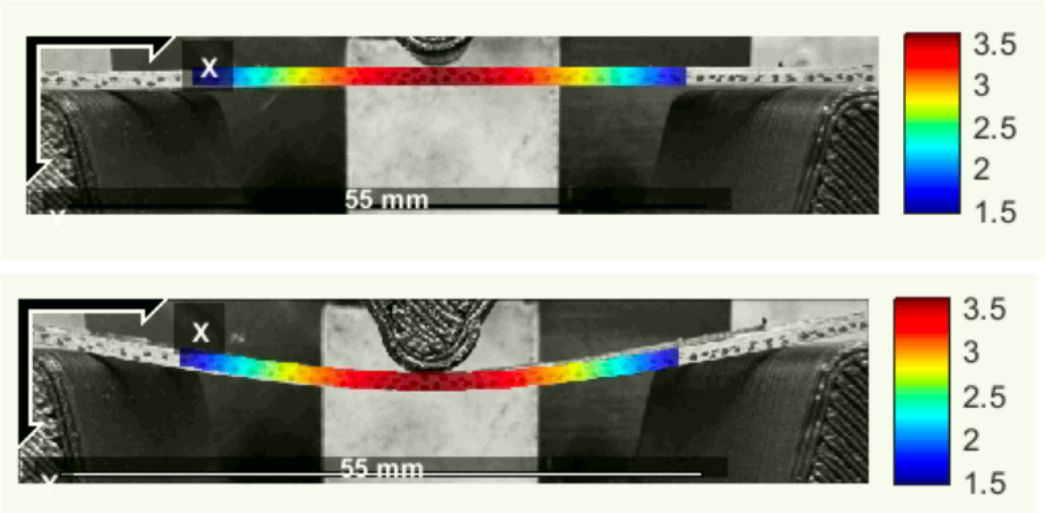

Figure 84 Y-axis displacement results in the reference image and in the deformed image

As seen in the images we can see that the expected result was obtained having a maximum displacement in the center of the specimen, where the load was applied, with a displacement of 3.5mm and approaching the minimum deformation as we go towards the supports. In this test, the region of interest was selected without reaching the supports, which results in the minimum displacement being 1.5mm in

the area furthest from the center in the region of interest but without reaching 0mm, which would be the expected deformation in the supports.

6.5.2 Strain Results

Once the displacement results have been analyzed, we can continue analyzing the results of the strains. It should be remembered that the results of the strains are dimensionless values but that they represent a proportion, that is, if in the graph we see a maximum point of 0.02 that means that we have 2% deformation.

The first result we have is horizontal deformation or EXX, which is possibly the most important strain result for a bending test because it shows us the tensile and compression values to which the specimen is subjected during the bending test. The expected result for this test will be to be able to see compression in the upper area of the specimen, and in the lower zone traction, due to the way in which the specimen deforms during the test.

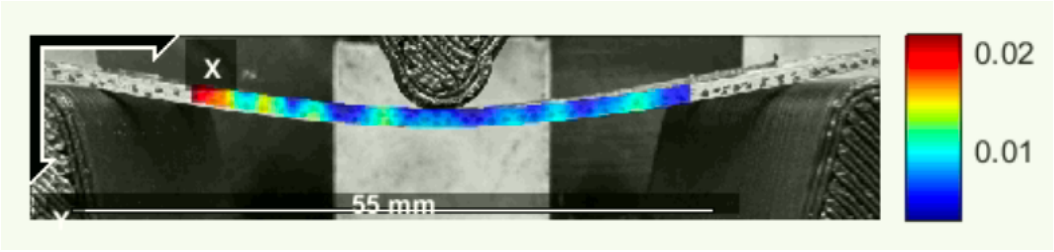

Figure 85 EXX: horizontal deformation.

In the image, we can see that the prediction holds true where we can see how there are more blue areas with less horizontal deformation in the upper part of the specimen compared to the lower part, where green spots appear, indicating an increase in deformation in that area. In other words, we can see that the lower part is more "stretched" and deformed than the upper part.

The following image shows the results of the shear strain or EXY. These results measure how the specimen changes shape or distort and the expected results of their analysis are values close to zero except for certain local areas, because pure bending behavior is expected since the specimen should only be stretched or compressed but not internal movement.

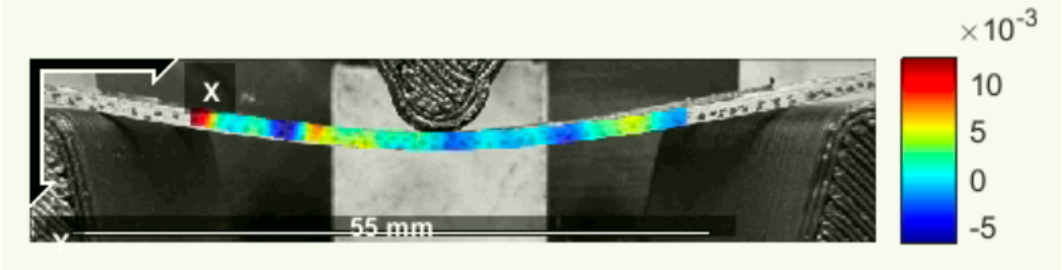

Figure 86 EXY: shear strain

As can be seen in the image, the strain inside the specimen is relatively uniform, with no mostly visible differences and with values very close to zero, so it can be said that we have about 0.1% of deformation per cut making it negligible and therefore the test is basically in pure bending. The hot points that can be seen with color peaks probably represent imperfections or noise during the tracking of the speckle pattern, since they are not areas near supports or areas near the load that could be generators of hot points.

Finally, we can finish the analysis of results with the last strain, which will be the vertical deformation or EYY. This strain measures how much the specimen is compressed or stretched in the direction perpendicular to the specimen, that mean. in the Y axis. The values obtained in this test would be expected to be significantly lower than those obtained in EXX.

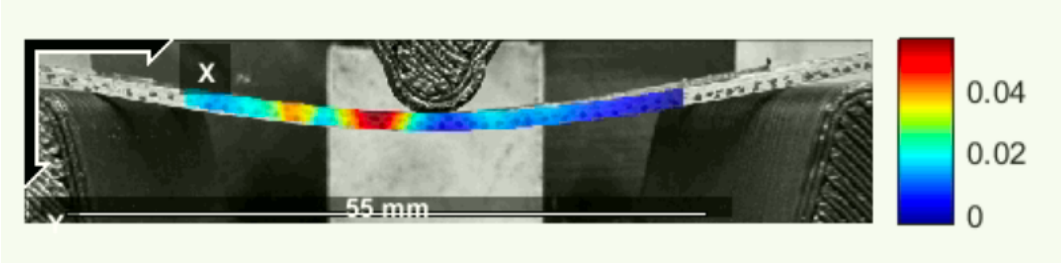

Figure 87 EYY: vertical deformation

In the image we can see a dominance of values very close to zero complying with what was expected; however, a large hot point is observed near the place where the load is applied that increases the average and exceeds the values obtained in EXX. This could be due to a local deformation in the specimen that was captured by the digital image correlation analysis or due to an error in the DIC analysis of the image, perhaps caused by a bad speckle pattern in that region that made the software aware of the presence of deformation or possible indentation on the part of the charging pin. However, these results can be taken as valid because in most of the result the specimen behaves as expected.

With all the results analyzed, it is worth mentioning possible sources of error in the results such as the presence of noise due to the quality of the speckle in the images and therefore small errors accumulated when tracing the speckle pattern. In the same way, the preprocessing we did to the images can lead to a certain level of error, mainly when passing the images through the threshold filter which by removing information from the image could have eliminated certain points that could have influenced during the tracking of the speckle pattern in the DIC analysis of the deformed images. Finally, it is also worth mentioning possible errors during the assembly of the test, such as the specimen not being correctly aligned on the supports or the loading pin not falling directly into the center of the specimen length.

6.5.3 Force Vs Displacement Chart

We now present the data obtained by the program made in LabVIEW which allowed us to obtain a graph of Force Vs Displacement in real time while performing the bending test. The data were exported and filtered from the complete set by cropping only to the initial section where the test began until the maximum deformation analyzed by digital image correlation, which was 3.5mm in the Y axis.

Table 2 Force and displacement data obtained during the bending test

Displacement [mm]	Force [N]
0	0
0,25	1,32
0,5	2,85
0,75	4,18
1	5,42
1,25	6,79
1,5	7,91
1,75	9,15
2	10,33
2,25	11,24
2,5	12,18
2,75	13,01
3	13,84
3,25	14,52
3,5	15,11

These values are graphed in Excel to obtain a cleaner dataset and a more ordered graph than the one obtained directly by the controller in LabVIEW.

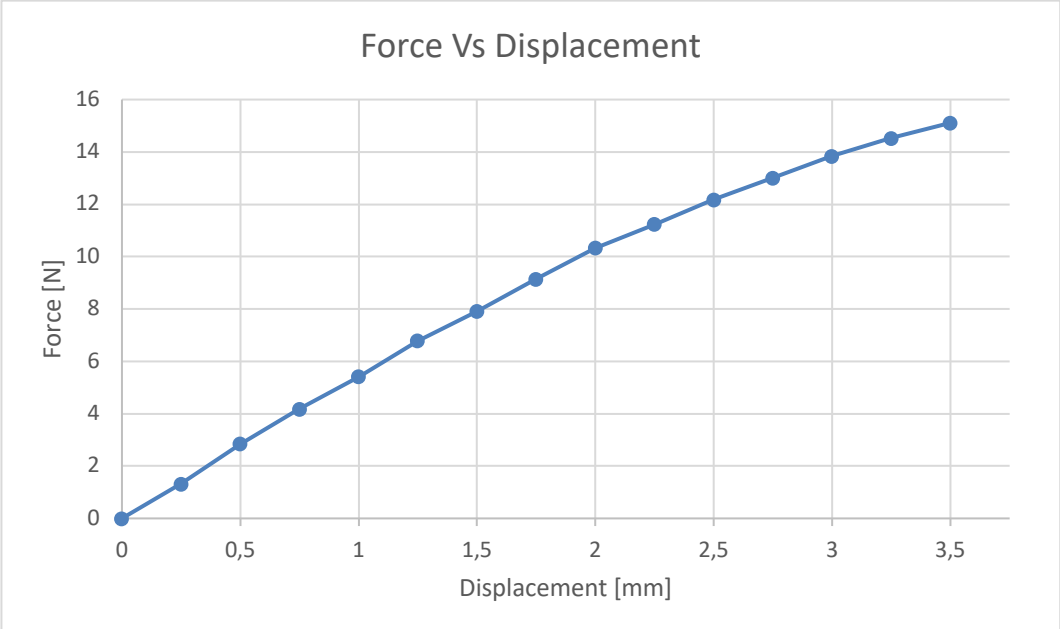

Figure 88 Force Vs Displacement Chart

As can be seen in the Force Vs Displacement graph, it can be observed how at the beginning of the curve it presents a linear elastic zone, or at least relatively linear

considering the noise of the sensor, until it reaches around 2mm of displacement where the curve begins to be more pronounced which represents a loss of linearity perhaps due to the presence of microcracks that begin to deform the material, until we continue to advance where the curve is more than evident, giving evidence that we are approaching its limit. However, in the figure we do not witness the limit because the test stopped at 3.5mm, which was the point of maximum deformation used for the analysis of digital image correlation, while the rupture of the specimen occurred later, so it was not recorded in the curve.

6.5.4 Other Machine Tests

In order to test the behavior of the machine with different materials, common materials were tested to see if the supports, the load pin and the machine in general were capable of taking measurements under other conditions. The specimens were designed according to the standard ASTM 790-17, in order to maintain quality in the results obtained.

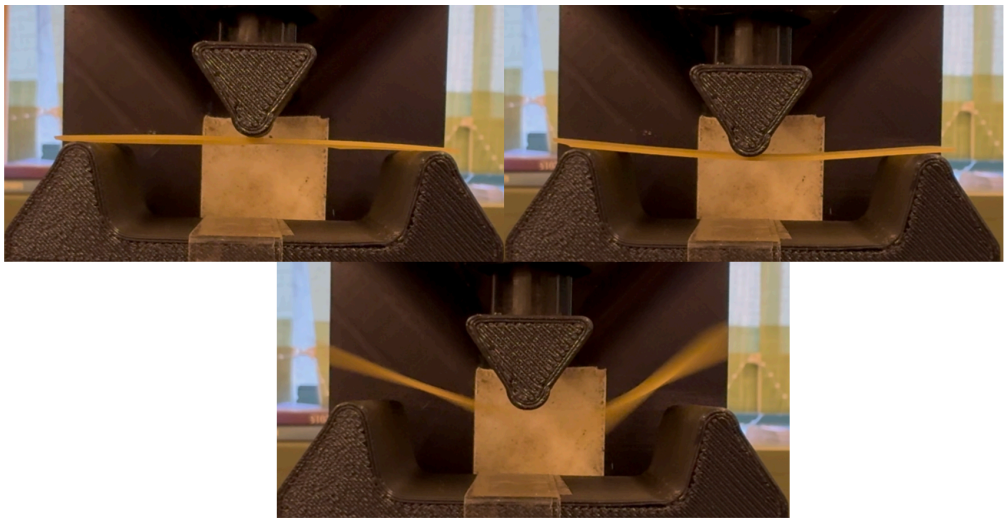

Figure 89 Bending test on flat pasta

In the image we can see the bending test on a specimen made of flat paste with dimensions of 60mm long, 0.8mm thick and 12.7mm wide. The paste presented a small deformation that could be measured with the machine, however, it did not stand the deformation and ended up breaking.

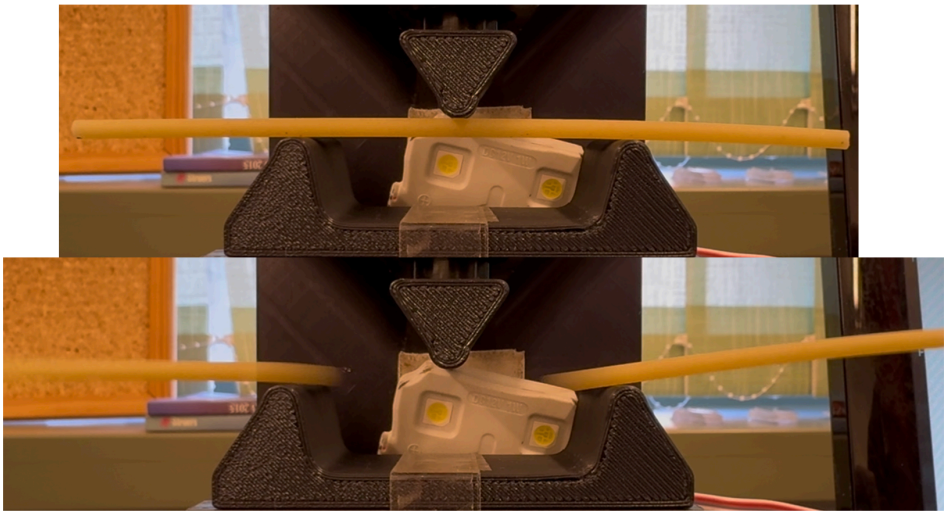

Figure 90 Bending test on spaghetti

In the same way, the machine was tested with a cylindrical specimen made of relatively thick spaghetti 127mm long, 12.7mm wide and a diameter of 3mm. According to the normative, if the thickness of the specimen is more than 3mm, the length becomes 127mm long instead of the 60mm with which the rest of the specimens were tested [18]. During the test, the specimen did not support the load from the beginning, so as soon as the load was applied, the specimen ended up splitting without being able to register any values in the machine due to the speed of the breakage.

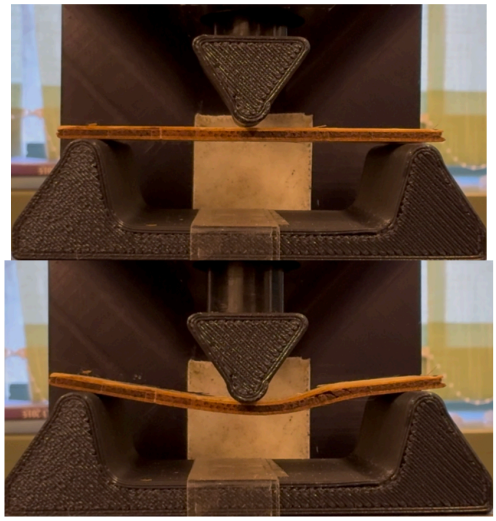

Figure 91 Bending test on chipboard

Finally, a specimen made of chipboard with dimensions of 60mm long, 2mm thick and 12.7mm wide was tested, with which very good results were obtained, being able to record values in real time in the Force Vs Displacement graph directly from the machine in LabVIEW and in case of wanting to do so, the thickness allowed to record a speckle pattern and to be able to perform a digital image

correlation analysis in Ncorr. We can see how the specimen flexed until it reached the point where it broke, however, we can see how the rupture was not in the center of the specimen as would be expected but went on one side towards one of the supports. This rupture could have been due to internal irregularities of the material made, considering that the specimen was made of agglomerate material, so internally its structure is not uniform.

7 Conclusions and Future Possibilities

To conclude this work, it is worth summarizing everything that has been done and learned during this project. The main objective of this study was to design a machine capable of performing three point bending tests in a reliably way and that in turn allows the obtaining of images of the tests performed and that these can be analyzed by optical techniques for measuring stress fields in a non invasive way and without contact with the sample that could alter the results of the analyses.

We began by analyzing the theory behind the bending test, which in turn includes studying the phenomenon of pure bending and all the mechanics that this includes. At the same time, we analyze how a three point testing machine works and learn the bases with which our prototype should comply.

In the same way, being a very standardized test and used in many areas as a tool to know and study the various materials with which we work, the bending test is highly standardized with which a previous study of the regulations that govern the test and therefore those that our test device, supports and specimens with which we are going to work must comply in order to obtain results that are valid and comparable to commercial grade testing machines.

With all the theory behind the study known and with a previous review of the current standards that support a good three point bending test, we can start designing the machine in question. For this we use controllers such as the NI myDAQ as the central axis of the machine, which will allow us to obtain analog data from the equipment during the tests, and in turn send digital signals that allow us to control the machine we design. A basic and robust system of controller, sensors, relays and motors is used which allows us to control the bending testing machine as we want through a program based on LabVIEW which we designed in such a way that with it we can control the machine safely and obtain some first results, such as the Force Vs Displacement graph, of our real time tests. The bending testing machine was designed so that it can handle a maximum load of 300N, enough for the tests we want to perform on fragile material such as glass or certain polymers.

Based on current regulations such as ASTM 790-17 for bending tests on plastics, the appropriate three-point supports were designed for the materials that were to be tested such as glass or other fragile materials, designing a base with supports with a 50mm span and 10mm diameter rollers, as well as a 10mm diameter load pin which will go in the middle of the base to apply force in the center of the specimen.

Based on the ASTM 790-17 standard, we can also design the appropriate specimens for our tests, which, being fragile materials, result in specimens of 127mm in length, with 12.7mm in width and a thickness of 3.2mm, being specimens that fit perfectly in the space that we have in the machine as a test space.

With all this ready, it was possible to build a functional bending testing machine which allows to apply controlled loads on the specimens and perform three point

bending tests, showing stability in their results and that these can be repeatable and validable with other specimens in new tests on the machine.

The objective of this work was to be able to measure stress fields in an optical way, so after analyzing several of the available techniques, it was decided to apply digital image correlation to our machine. Therefore, the respective normative was first sought to be able to execute DIC practices adequately in bending tests and base ourselves on the manual of *"A Good Practices Guide for Digital Image Correlation Standardization, Good Practices, and Uncertainty Quantification Committee"*, by International Digital Image Correlation Society (iDICs), we were able to determine the right conditions that our system must have in order to be able to perform a Digital Image Correlation analysis properly.

It was decided to use a 2D DIC system, so that a single camera is sufficient for image acquisition during the bending test. In this case, a Sony Cybershot DSC-QX10 was used, which would be controlled wirelessly from the computer to obtain good quality images during the test. At the same time, a good lighting system was required, so a configuration of a white LED light connected to a potentiometer was used, from which the intensity of the light can be configured and the appropriate one can be selected for our test that allows us to ensure good image quality and good contrast in the speckle pattern, which is crucial to perform digital image correlation.

As mentioned, a good speckle pattern is required to be able to perform digital image correlation, for which we rely on the manual of a good application of the speckle pattern by Correlated Solutions. With this in mind we make sure to apply a speckle pattern on the flat surface of the specimen that we want to study, respecting that these are uniform random points in size, with a density of 50-50 with respect to the background, using a matte black color that allows a good contrast of image without reflecting due to direct lighting and that can alter the image or cause unnecessary noise, And most importantly, an ideal speckle pattern without deformations in its points or lines or unwanted blur that makes it difficult to track the points in Digital Image Correlation's analysis software.

Finally, the images obtained were preprocessed using ImageJ where we cropped the images by removing unnecessary information and isolating only the flexural test area, applying a threshold filter to black and white in order to increase the contrast and eliminate unnecessary information in the image, and transforming the image to 8-bit format, image in RGB format and exporting them in .tiff format in order to ensure total compatibility with the Digital Image Correlation analysis software we use.

In order to maintain a philosophy of simplicity and to go straight to the result we want, we opted directly to use an opensource software for digital image correlation analysis called Ncorr, which is a program that runs on MATLAB and allows us to perform DIC in a reliable and free way because the software is validated by studios and compared with specialized commercial software for DIC. Using Ncorr we can select the region of interest of the images we load, both in their reference image and in the images deformed during the bending test, and by configuring a good subset

to track points and pixels in the sequence of images, we can obtain results of displacements and strains in Ncorr. In the same way we can calibrate a scale in the images to obtain results in the units we want, in our case the images were scaled to mm.

Finally, using Ncorr, we obtained results of complete fields of displacement and deformation from the images we took during the bending test. The analysis of the results demonstrated good performance of the specimens, returning the expected data and consistent with what would be expected from a three-point bending test. Obtaining a maximum displacement in the center of the specimen where the load was applied of 3.5mm on the Y axis and 0.6mm on the X axis, which are consistent results with what should be obtained from a bending test. Similarly, in the analysis of strains we obtained the expected distribution of compression and traction on the specimen, as well as the vertical and horizontal deformations presented expected results of this type of tests.

Concluding that the bending testing machine built, together with the supports and specimens designed based on international standards; and the procedure followed to obtain images and preprocess them to perform a Digital Image Correlation analysis was adequate, obtaining decent, comparable and validable results; allowing us to use the machine for future bending tests in various material analyses ensuring that your results will be adequate.

Based on the work carried out, certain lines of improvement can be seen for possible future work, which would allow a greater scope in the capabilities of the designed machine. Starting from the fact that the load capacity of the machine can be increased, because 300N is sufficient for micro scale analysis and with fragile materials, but not with materials generally used in engineering such as plastics and metals. For this, the base of the supports and therefore the load pin must be redesigned, making it more robust. In the same way, it was planned to make a version of the base with interchangeable supports for a greater variety of tests.

Similarly, a more robust calibration system could be applied using strain gauges to ensure proper calibration and to reduce noise in the results obtained in real time during the flexural test.

It is worth mentioning that an attempt could be made to expand the scope of the analysis by implementing another camera to be able to perform 3D DIC analysis, thus obtaining 3D analysis results that allow to show more completely the behavior of the specimens or studio bodies.

Similarly, at the software level, the interface designed in LabVIEW could be improved, making it even more intuitive and with more options such as an emergency stop button on the machine or with the option of several graphs that it shows us during the test. Another program could also be implemented, or implemented directly in the same program made in LabVIEW by integrating image acquisition and analysis directly there; which allows a more adequate and simple pre-processing of the images, possibly applying a macros in ImageJ or from a code

in MATLAB, which allows loading the sequence of images and giving us a set of images ready to perform the analysis of digital image correlation.

Finally, we could try more software options, opensource or commercial, which could give us more options for results such as other types of graphics or 3D images, further expanding the range of possibilities for bending test studies with the machine we have designed.

List of references/Bibliography

[1] Hibbeler, R. C.: *Mechanics of Materials, Tenth Edition*, Pearson Education, Inc., Harlow, 2018. ISBN 10: 1-292-17820-5.

[2] Ingeniosos: Esfuerzo de flexion, In: Lawebdeingeniosos {online} https://lawebdeingeniosos.com/esfuerzo-de-flexion/ (Accessed 4.12.2025, 4:20 p.m.)

[3] Ingeniosos: Segundo momento de inercia ¿Que es y como calcularlo?, In: Youtube {online} https://www.youtube.com/watch?v=3DKBcdGo9Ok (Accessed 4.12.2025, 6:30 p.m.)

[4] Instron España.: ¿Qué es un ensayo de flexion?, In: Youtube {online} https://www.youtube.com/watch?v=T1jAEq7PeoY (Accessed 5.12.2025, 8 a.m.)

[5] Instron: 2810 SERIES MINI FLEXURE FIXTURE. Catalog Numbers 2810-412, 413. Instron, Norwood, 2022.

[6] Ingeniosos: ¿Qué es el ensayo de flexion?, In: Youtube {online} https://www.youtube.com/watch?v=AiCbX1KXEfs (Accessed 5.12.2025, 2 p.m.)

[7] Triangle Engineering: Everything You Need to Know about Guided Bend Testing of Welds, Destructive weld testing, In: Trieng {online} https://trieng.com/blogs/resources/bend-test-welding-complete-guide?srsltid=AfmBOoqvRLR3pnuFMeRJZjXZPGDRLaYqExJmaA0G7Qn_kMcvjdye8Xv8 (Accessed 10.12.2025, 2:52 p.m.)

[8] Alarcón, O. E., Medrano, M. E. and Gillis, P.P.: Fracture of glass in tensile and bending tests, In: Metallurgical and Materials Transactions A, 1994, vol. 25(5), pp. 961–968, DOI: 10.1007/bf02652271

[9] Maniatis, I., Nehring, G., & Siebert, G.: Studies on determining the bending strength of thin glass, In: Proceedings of the Institution of Civil Engineers - Structures and Buildings, 2016, vol 169(6), pp. 393–402, https://doi.org/10.1680/jstbu.14.00003

[10] Vedrtnam, A., & Pawar, S.: Experimental and simulation studies on flexural strength of laminated glass using ring-on-ring and three-point bending test, In: Proceedings of the Institution of Mechanical Engineers, Part C: Journal of Mechanical Engineering Science, 2017, vol 232(21), pp. 3930–3941, https://doi.org/10.1177/0954406217744815

[11] Almaguer, Z. PM., Zambrano, R. P., Martínez, G. de P. JA., et al.: Evaluación a fractura de probetas de sección transversal cuadrada solicitadas a torsión cíclica, Ingeniería Mecánica, 2019, vol 22(3), pp. 142-149, ISSN 1815-5944.

[12] Torres, D. A., et al.: Ensayo de flexion, In: Researchgate {online} https://www.researchgate.net/publication/328550903_ENSAYO_DE_FLEXION (Accessed 8.12.2025, 2 p.m.)

[13] Sotelo, M. A. R., Ensayo de Flexión. In: Scribd {online} https://es.scribd.com/document/381421195/Ensayo-de-Flexion (Accessed 8.12.2025, 4 p.m.)

[14] Mecmesin, Flexión, In: mecmesin {online} https://www.mecmesin.com/es/test-type/flexure (Accessed 10.12.2025, 6:30 p.m.)

[15] Instron: Ensayo de Flexión Una introducción, In: Instron {online} https://www.instron.com/es/resources/test-types/flexural-testing/ (Accessed 2.12.2025, 7 p.m.)

[16] Instron España, ¿Qué es una máquina universal de ensayos?, In: Youtube {online} https://www.youtube.com/watch?v=mHzwXv64Iac (Accessed 9.12.2025, 10 a.m.)

[17] BS EN ISO 178:2019. Plastics - Determination of flexural properties, In force from: May 2019, BSI Standards Publication, Londres, 2019.

[18] ASTM D790-17. Standard Test Methods for Flexural Properties of Unreinforced and Reinforced Plastics and Electrical Insulating Materials, In force from: 1 July 2017, ASTM International, West Conshohocken, 2017.

[19] Gao, G., Huang, S., Xia, K., Li, Z.: Application of Digital Image Correlation (DIC) in Dynamic Notched Semi-Circular Bend (NSCB) Tests, In: Experimental Mechanics, 2014, DOI 10.1007/s11340-014-9863-5.

[20] Instron: 2810 SERIES MICRO 3-POINT BEND FIXTURE. Catalog Numbers 2810-410, 411. Instron, Norwood, 2021.

[21] Briñez, J. C., Restrepo, A., López, F.: Estudios de Fotoelasticidad: Desarollos y Aplicaciones, In: Revista Politécnica, 2013, vol 16(9), pp. 27-36. ISSN 1900-2351.

[22] Alcaraz, A.: Prototipo Optomecatrónico Basado en Holografía Digital Interferometrica Orientado al Estudio de Tejidos Biológicos. In: cio.repositorioinstitucional {online} https://cio.repositorioinstitucional.mx/jspui/bitstream/1002/576/1/15705.pdf (Accessed 8.12.2025, 10 p.m.)

[23] Vera, D.: *La Técnica de Correlación de Imágenes Digitales Aplicada a Ensayos de Materiales*, Pontificia Universidad Catolica del Peru, Lima, 2020, http://hdl.handle.net/20.500.12404/17193

[24] International Digital Image Correlation Society, Jones, E.M.C. and Iadicola, M.A. (Eds.) (2018). A Good Practices Guide for Digital Image Correlation. https://doi.org/10.32720/idics/gpg.ed1/print.format.

[25] Carlosz22, Polarimetria casera - Técnicas de fotoelasticidad, In: Youtube {online} https://www.youtube.com/watch?v=DTYRByCY7Go (Accessed 3.02.2025, 10 a.m.)

[26] Universitat Politécnica de Valéncia - UPV, Análisis de tensiones mediante fotoelasticidad || UPV, In: Youtube {online} https://www.youtube.com/watch?v=bZtEns1iG6M (Accessed 3.02.2025, 11 a.m.)

[27] Inte Urango, J.C., Carmen, G., Briñez, J.C., Restrepo-Martínez A.: Validación del uso de fotoelasticidad como herramienta para los cursos de Mecánica de Sólidos, In: Revista EIA, 2017, vol 14(28), pp. 117-131, https://doi.org/10.24050/reia.v14i28.1145

[28] Wei, Shan, Pang, Yajun, Bai, Zhenxu, Wang, Yulei, Lu, Zhiwei: Research Progress of Stress Measurement Technologies for Optical Elements, In: International Journal of Optics, 2021, 5541358, 11 pages, 2021. https://doi.org/10.1155/2021/5541358

[29] W. H. Peters, W. F. Ranson, M. A. Sutton, T. C. Chu, J. Anderson: Application of digital correlation methods to rigid body mechanics, In: Optical Engineering, 1983, vol 22(6), pp. 738-742

[30] European Structural Integrity Society, Crack Closure Phenomenon by Electronic Speckle Pattern Interferometry, In: Youtube {online} https://www.youtube.com/watch?v=DI-EGyJG7UI (Accessed 4.02.2025, 16 a.m.)

[31] Román, Juan & Fernández, P & Moreno, Vicente & Abeleira, Maite & Gallas-Torreira, Mercedes & Suarez, Daniela: The mechanical behaviour of human mandibles studied by electronic speckle pattern interferometry. In: European journal of orthodontics, 1999, vol 21, pp. 413-21, DOI:10.1093/ejo/21.4.413.

[32] Mousa, M.A. Yussof, M.M. Hussein, T.S. Assi, L.N. Ghahari, S.: A Digital Image Correlation Technique for Laboratory Structural Tests and Applications: A Systematic Literature Review. In: Sensors 2023, 23, 9362, https://doi.org/10.3390/s23239362

[33] Eberl, C. Gianola, D. S. Hemker, K. J.: Mechanical Characterization of Coatings Using Microbeam Bending and Digital Image Correlation Techniques. In: Experimental Mechanics, 2010, vol 50, pp. 85–97, DOI:10.1007/s11340-008-9187-4

[34] Ramos, T. Braga, D. Eslami, S. Tavares, P. Moreira, P.: (2015). Comparison Between Finite Element Method Simulation, Digital Image Correlation and Strain Gauges Measurements in a 3-Point Bending Flexural Test. In: Procedia Engineering, 2015, vol 114, pp. 232-239, DOI:10.1016/j.proeng.2015.08.063.

[35] Siemens Software, WHAT'S NEW Digital Image Correlation (DIC) for materials and structural testing, In: Youtube {online} https://www.youtube.com/watch?v=jHM-1XYyRiU (Accessed 7.02.2025, 12 p.m.)

[36] Pan, B.: Digital image correlation for surface deformation measurement: historical developments, recent advances and future goals, In: Measurement Science and Technology, 2018, vol 29, no. 8, p. 082001, DOI: 10.1088/1361-6501/aac55b.

[37] Correlated Solutions, Fundamentals of Speckling for DIC, In: Youtube {online} https://www.youtube.com/watch?v=z9QHc5K4X4A (Accessed 23.02.2025, 16 p.m.)

[38] Shimadzu, Material Testing by Strain Distribution Visualization – DIC Analysis –, In: Shimadzu Application News, 2012, No.i247, LAAN-A-AG-E012.

[39] Blaber, J. Antoniou, A.: Ncorr Instruction Manual Version 1.2.2, Georgia Institute of Technology, 2017.